AD NUMBER

AD870778

LIMITATION CHANGES

TO:

Approved for public release; distribution is unlimited.

FROM:

Distribution authorized to U.S. Gov't. agencies and their contractors; Critical Technology; 27 APR 1970. Other requests shall be referred to Air Force Technical Applications Center, Washington, DC 20333. This document contains export-controlled technical data.

AUTHORITY

USAF ltr, 25 Jan 1972

AFTAC Project No. VELA/T/0701/B/ASD

A PRELIMINARY STUDY OF TECHNIQUES FOR ROUTINE MATCHED FILTERING OF SURFACE WAVES

Technical Report No. 4

SEISMIC ARRAY PROCESSING TECHNIQUES

Prepared by

Frank H. Binder

Stanley J. Laster, Project Scientist
Frank H. Binder, Program Manager
Area Code 214, 238-6521

TEXAS INSTRUMENTS INCORPORATED
Services Group
P.O. Box 5621
Dallas, Texas 75222

Contract No. F33657-70-C-0100
Amount of Contract: $339,052
Beginning 15 July 1969
Ending 14 July 1970

Prepared for

AIR FORCE TECHNICAL APPLICATIONS CENTER
Washington, D. C. 20333

Sponsored by

ADVANCED RESEARCH PROJECTS AGENCY
Nuclear Monitoring Research Office
ARPA Order No. 624
ARPA Program Code No. 9F10

27 April 1970

Acknowledgment: This research was supported by the Advanced Research Projects Agency, Nuclear Monitoring Research Office, under Project VELA-UNIFORM, and accomplished under the technical direction of the Air Force Technical Applications Center under Contract No. F33657-70-C-0100.

AFTAC Project No. VELA/T/0701/B/ASD

A PRELIMINARY STUDY OF TECHNIQUES FOR ROUTINE MATCHED FILTERING OF SURFACE WAVES

Technical Report No. 4

SEISMIC ARRAY PROCESSING TECHNIQUES

Prepared by

Frank H. Binder

Stanley J. Laster, Project Scientist
Frank H. Binder, Program Manager
Area Code 214, 238-6521

TEXAS INSTRUMENTS INCORPORATED
Services Group
P.O. Box 5621
Dallas, Texas 75222

Contract No. F33657-70-C-0100
Amount of Contract: $339,052
Beginning 15 July 1969
Ending 14 July 1970

Prepared for

AIR FORCE TECHNICAL APPLICATIONS CENTER
Washington, D. C. 20333

Sponsored by

ADVANCED RESEARCH PROJECTS AGENCY
Nuclear Monitoring Research Office
ARPA Order No. 624
ARPA Program Code No. 9F10

27 April 1970

Acknowledgment: This research was supported by the Advanced Research Projects Agency, Nuclear Monitoring Research Office, under Project VELA-UNIFORM, and accomplished under the technical direction of the Air Force Technical Applications Center under Contract No. F33657-70-C-0100.

This document is subject to special export controls and each transmittal to foreign governments or foreign nationals may be made only with prior approval of Chief, AFTAC.

Qualified users may request copies of this document from:

Defense Documentation Center
Cameron Station
Alexandria, Virginia 22314

TABLE OF CONTENTS

LIST OF ILLUSTRATIONS

LIST OF TABLES

SUMMARY

This report discusses the study made on the effectiveness of various matched filters for processing surface waves of events in the Kuriles as recorded at LASA. The correlation coefficients and signal-to-noise improvements are presented for matching waveforms which include master events, a chirp waveform, and waveforms generated from crustal models. Based on the results of this study, procedures are recommended for implementation of large scale matched filtering at the SAAC center.

BLANK PAGE

SECTION I

INTRODUCTION

The purpose of this study was to investigate the practical problems encountered when trying to implement matched filter routinely on large numbers of events. The most important consideration relative to large scale implementation is the choice of the matching waveform.

In choosing a matching waveform, the net gain, in terms of more useful output, must be balanced in terms of the effort required. Any procedure for choosing the matching waveform must be logically simple enough to eliminate the need for human judgement.

The answer to this basic question is considered to be dependent upon the source region and the nature of the crustal path between source and receiver. This study was conducted using 17 earthquakes in the Kuriles-Kamchitka region and recorded at the Montana LASA. Conclusions drawn from these data are probably not applicable to other source regions and recording stations; however, they do serve as an initial guide to wholesale processing of Rayleigh and Love wavetrains.

Two basic types of matching waveforms were used in conducting this study:

- Master events – These are well recorded events from the same source region. An important consideration is how close the master event must be to the test event, as this governs the storage and searching required for general implementation. The master events were chosen to give a good sampling of epicentral separations.

- Synthetic waveforms – These were generated from crustal models. A simple radar-type Chirp (linear increase of frequency through time and uniform amplitude) was also used.

These waveforms were then used to do matched filtering using the ensemble of events. Correlation coefficients and signal-to-noise (S/N) improvements in random noise were calculated. Finally these data were used to make recommendations about batch processing using matched filtering.

The information contained in each section of this report is: Section II-brief recapitulation of the matched filtering concept; Section III-detailed description of the data used in the study and discussion of the implications of this data to the conclusions; Section IV-detail discussion of the results obtained. The conclusions are largely subjective; therefore, the experimental results are presented in great detail for the interested reader to examine; Section V-conclusions which the author considers pertinent to large volume, automated, matched filtering resulting from examination of the data and results.

SECTION II

MATCHED FILTERING CONCEPTS

Matched filtering is a convolution of a matching waveform with the signal-plus-noise channel. The "best" matching waveform is the time inverse of the signal waveform itself. It can be shown that, under the most generally accepted criterion of goodness, the optimum linear filter is shown by the equation

$$\text{optimum linear filter} = \Phi^{-1}V \qquad \text{(II-1)}$$

where Φ^{-1} is the inverse of the noise correlation matrix and V is the signal waveform. (This assumes, obviously, that a prior knowledge of the signal waveform exists).

In application to processing of seismic surface waves the Φ^{-1} part of the optimum linear filter has been eliminated and some estimate of the surface wavetrain has been used. Studies* conducted indicate that this procedure causes a negligable loss as compared with the optimum linear filter.

For random noise, which has the same bandwidth as the signal, it can be shown that matched filtering using the signal waveform which is of uniform amplitude would give a gain in S/N ratio of the time duration - bandwidth product. The S/N ratio being defined as

$$S/N = \frac{(\text{Max signal amp})^2}{\text{Average Mean Square Noise}} \qquad \text{(II-2)}$$

---

* Lincoln Lab Test Note 1967-50, 1967, Long-period signal processing results for large aperature seismic array, Nov 15.

BLANK PAGE

SECTION III

DESCRIPTION OF SUBJECT EVENTS

The epicenter, depth, magnitude, back azimuth, and distance from LASA for the 17 events used in the study are shown in Table III-1. Three things of special note are

- All the events are near magnitude 5. This should help eliminate great differences in spectral content due to source characteristics, and should give a good S/N ratio on a LASA beam.
- All the events are shallow. Deep events should be eliminated from LP processing for discrimination by detection of depth phases from short-period stations. This also eliminates another possible difference in surface wavetrain characteristics due to source mechanisms.
- All the events have a back azimuth of about 310 to 315° from LASA. This means the surface waves are traveling along the continent-ocean basin boundary over most of their path. This path could possibly result in anomalously rapid changes in waveform as a function of epicenter (the path suggests a complicated multipath situation).

The geographical locations of the epicenters of the events are shown in Figure III-1. It is included to help orient the reader with respect to major physiographic features.

The LASA beam outputs (vertical traces) for each event are shown in Figure III-2. The events have not been equally scaled in this figure, and have been hand traced. This imposed some unnatural angularity to the waveforms.

Table III-1

EVENT SUMMARY

Event	Long	Lat	Depth	M_b	Δ	Az
1016	150.2E	44.6N	33	4.7	66.9	311°
1018	140.9E	35.6N	59	5.3	78.6	310.3°
1019	160.4E	52.5N	33	4.8	56.9	312.8°
1131	147.2	43.5	36	5.7	69.2	311.8
1141	147.7	43.3	12	5.3	69.1	311.3
1142	147.7	43.3	33	5.1	69.1	311.3
2008	152.5	46.7	40	5.6	64.3	311.5
2010	151.7	44.3	26	5.8	66.3	310.6
2017	151.4	45.5	41	5.5	64.8	311.4
2018	152.0	46.3	40	5.5	64.8	311.4
2019	151.8	45.7	40	5.9	65.3	311.8
2020	149.5	45.2	23	5.4	65.3	311.2
2027	155.4	47.5	29	5.2	62.3	311.1
2028	150.7	45.4	33	5.3	66.1	311.4
2029	154.4	49.1	33	5.3	60.7	312.7
2032	160.4E	54.6N	33	5.5	55.5	315.2°
2033	157.7	51.2	24	5.5	58.8	313

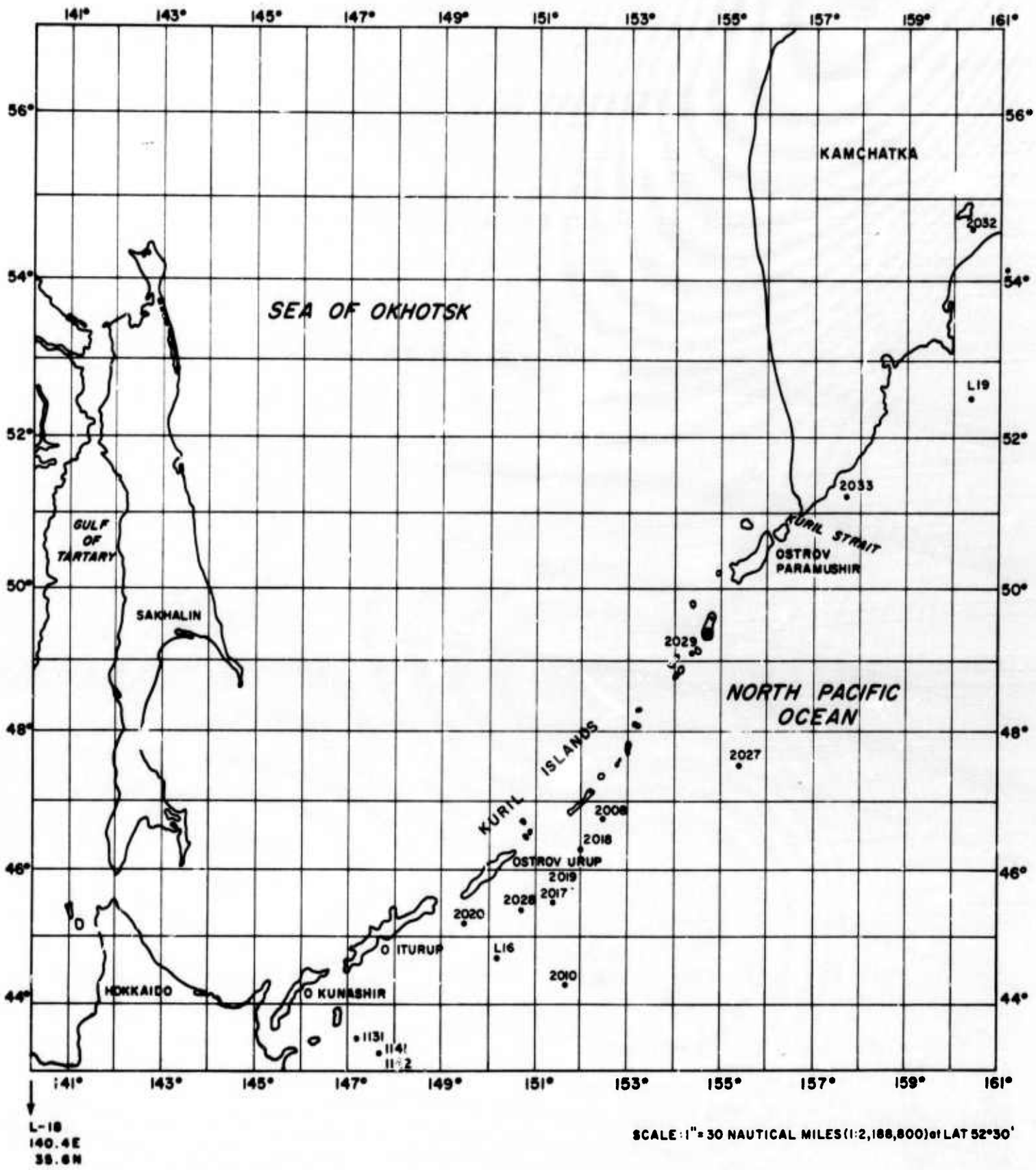

Figure III-1. Geographical Locations of Epicenter of Events

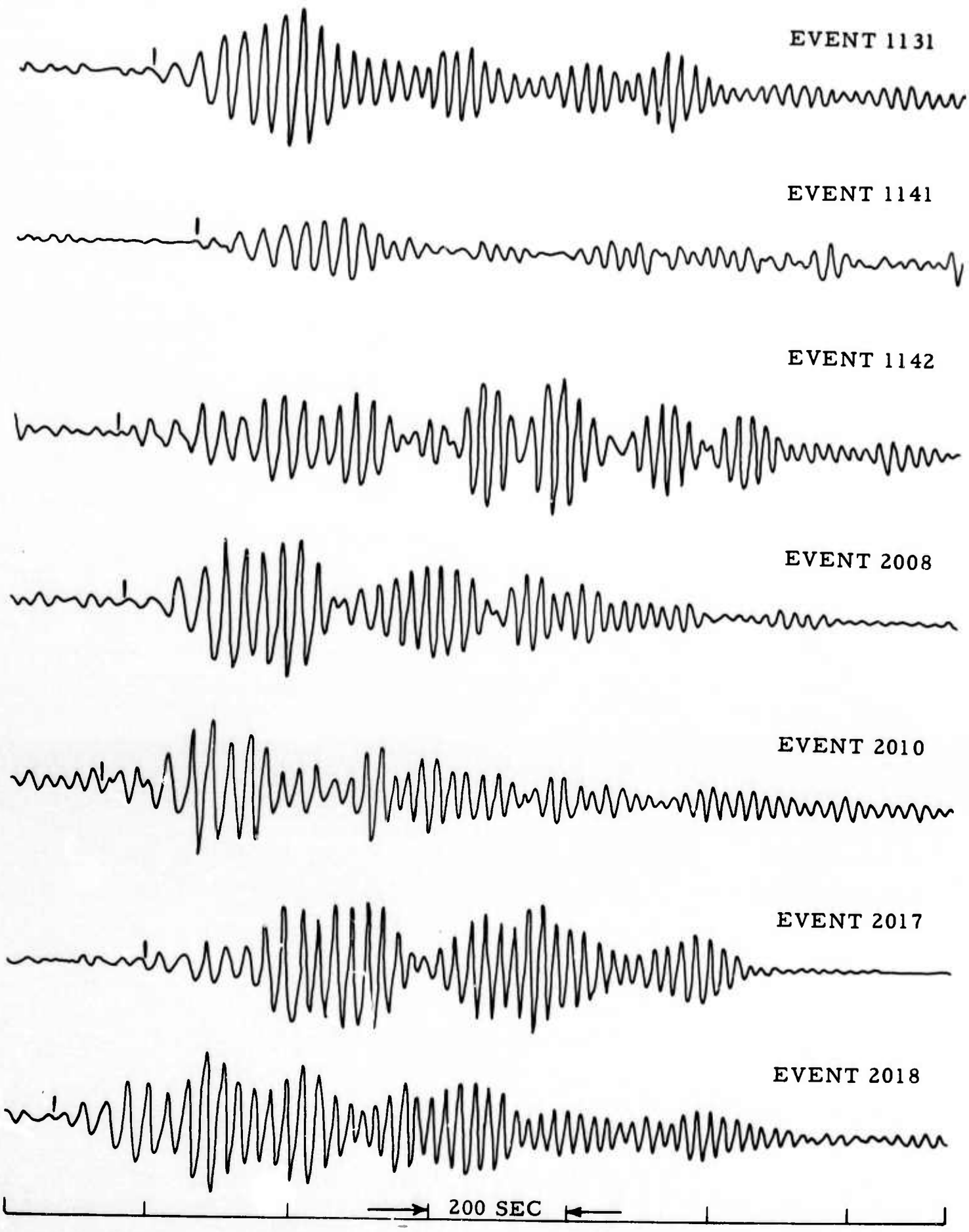

Figure III-2. Vertical Traces of LASA Beam Output of Each Event (Sheet 1 of 3)

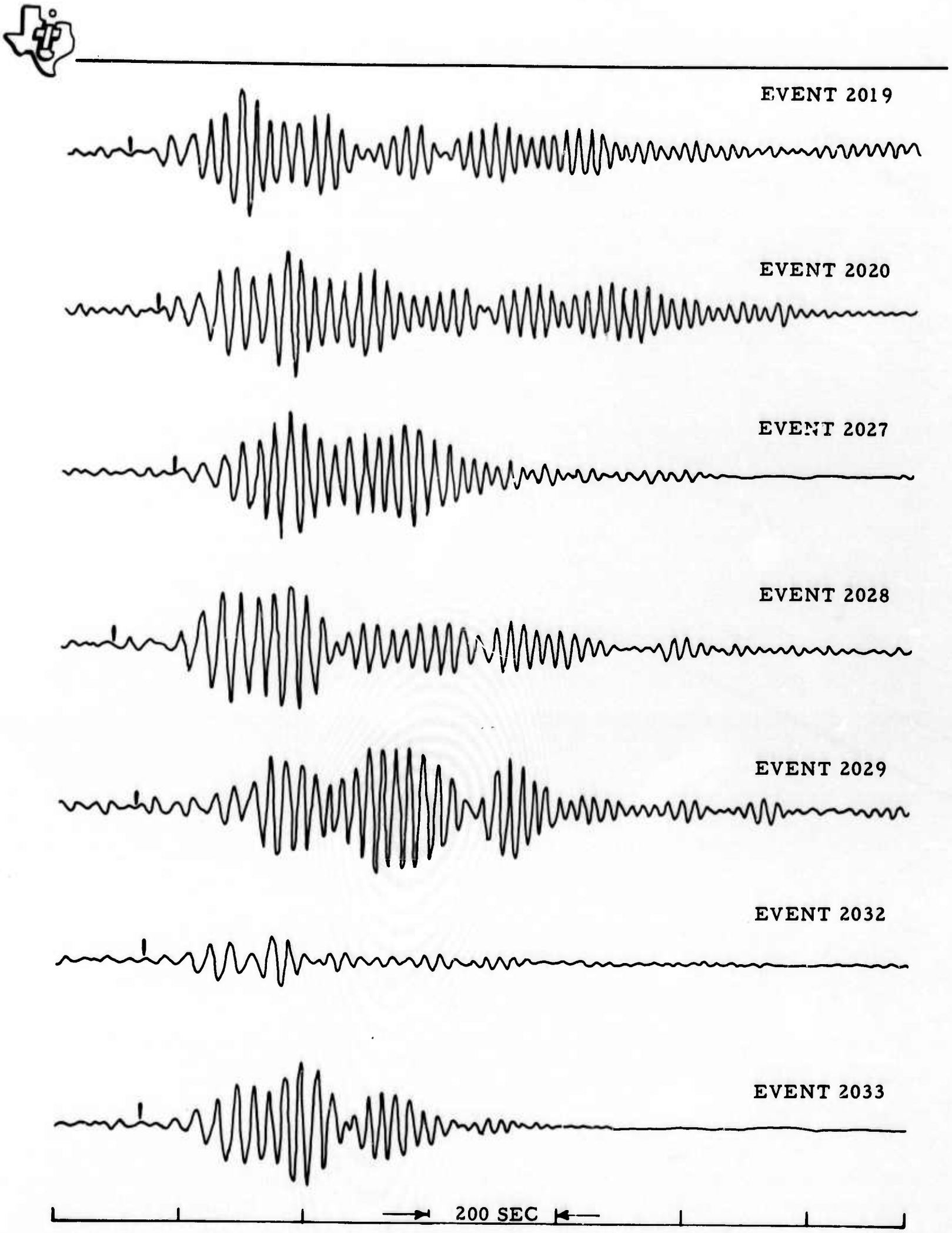

Figure III-2. Sheet 2 of 3.

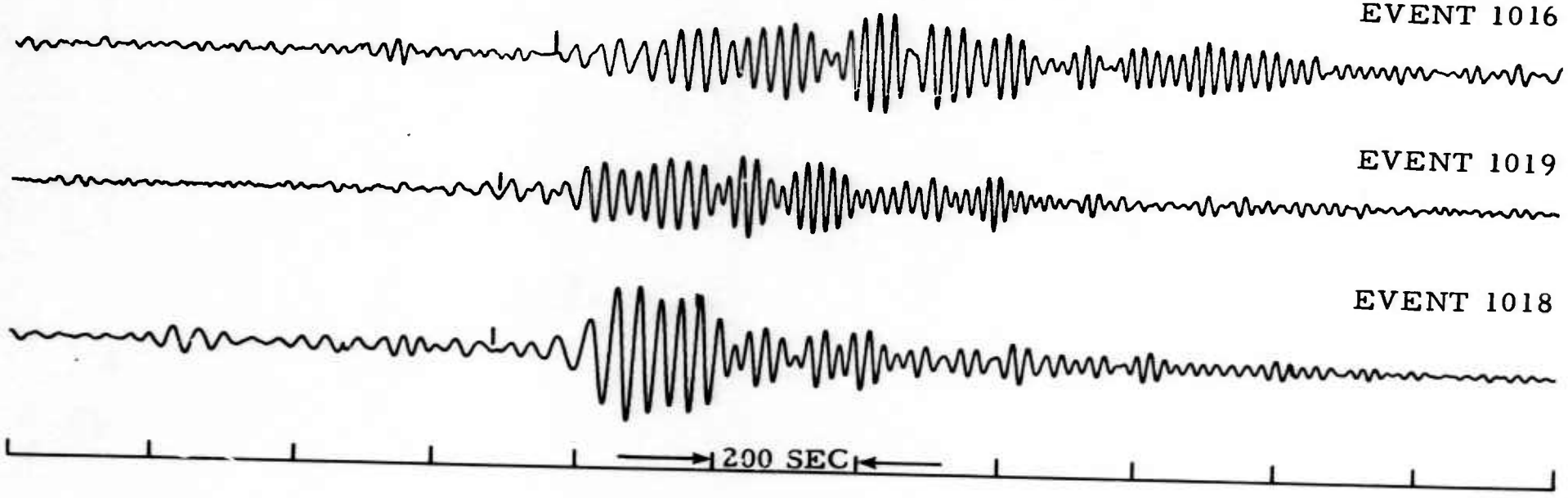

Figure III-2. Sheet 3 of 3.

The following features of data shown in Figure III-2 are considered pertinent:

- The events all have a very good S/N ratio. This may not be so obvious on some events as the time trace has been cut off and shows only a gate where signal energy is present.
- The simplier events (such as 2033 for example) have the great majority of their energy in the first 500 seconds after onset. Crustal models suggest that at 60 to 70° distance, a Rayleigh wavetrain from an impulsive source, with the bandwidths observed for these events, should die out in about 400 seconds.
- The events' waveforms are quite variable. Many of the events are highly modulated and many have a considerable coda of energy which is persistent long beyond 500 seconds.

Figure III-3 shows the amplitude spectra of the events as seen through the LASA LP instrumentation. Shown are spectra from the first 300, 512, and 1024 seconds of the analysis gate which indicate:

- With the exception of event 1019, the energy in these events is generally limited to the 0.025- to 0.05-Hz band (20- to 40-sec periods).
- These spectra were used to estimate an average bandwidth for each gate (300, 500, and 1024 sec). This average number listed below, was used for all events in the calculation of S/N improvements contained in Section IV:

300 sec	0.015 Hz
512 sec	0.019 Hz
1024 sec	0.021 Hz

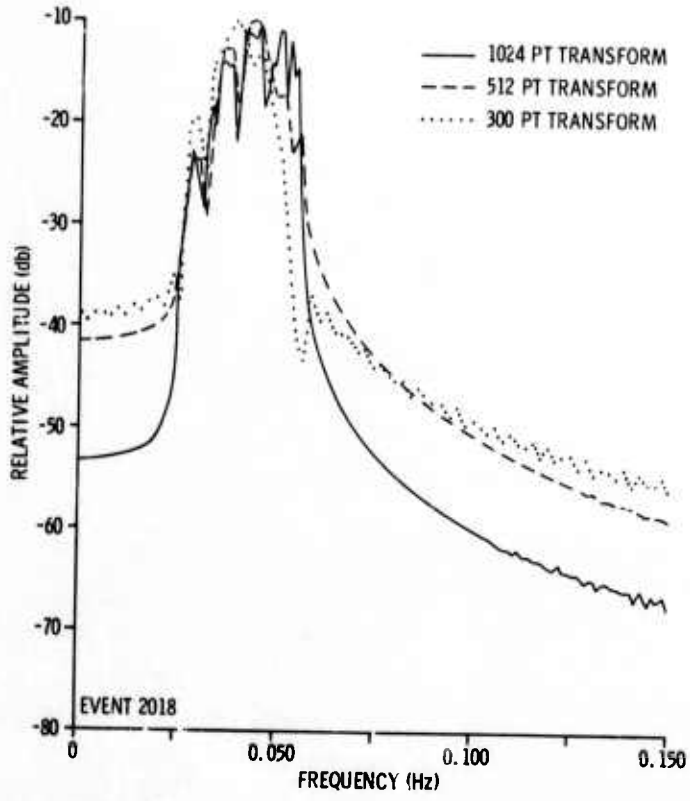

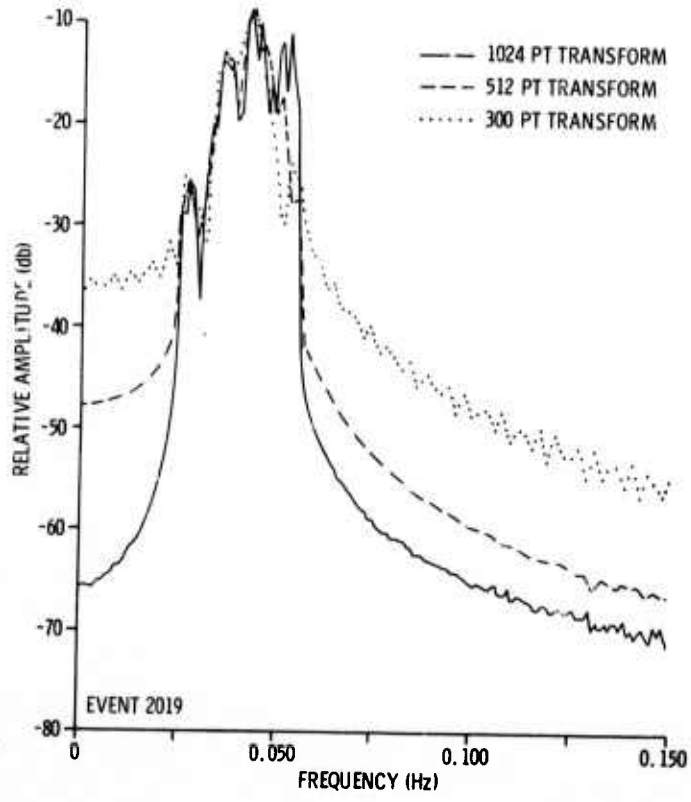

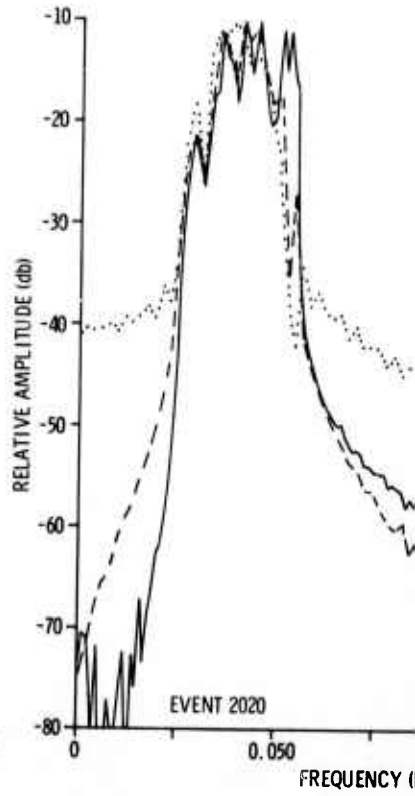

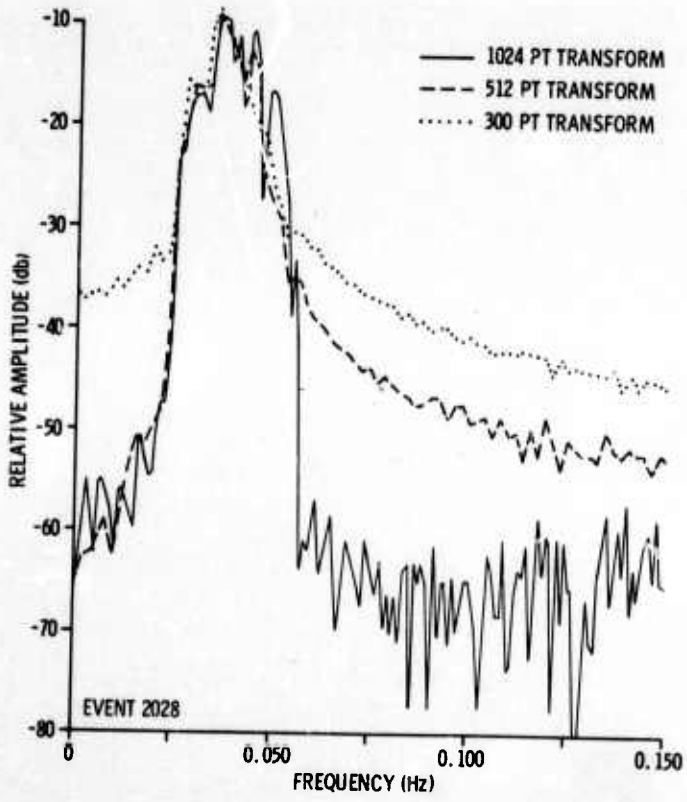

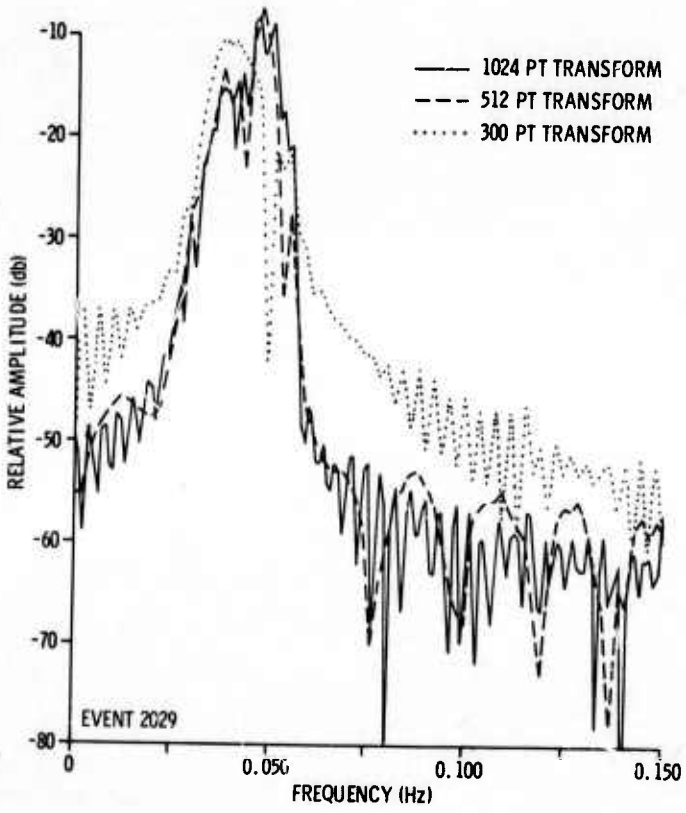

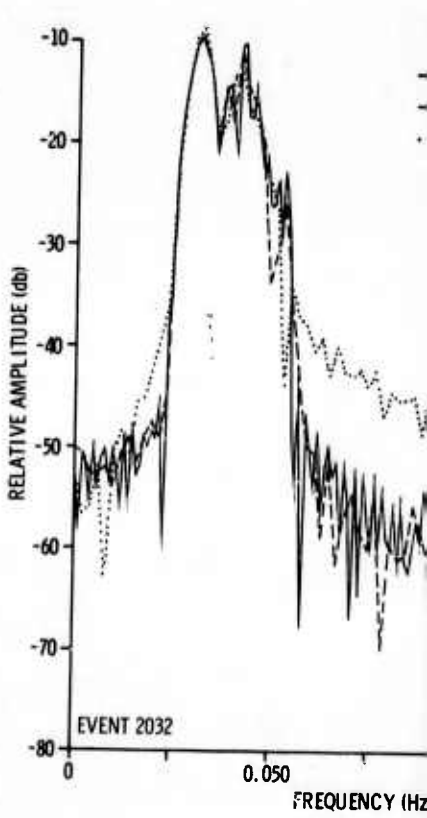

Figure III-3. A
T

A

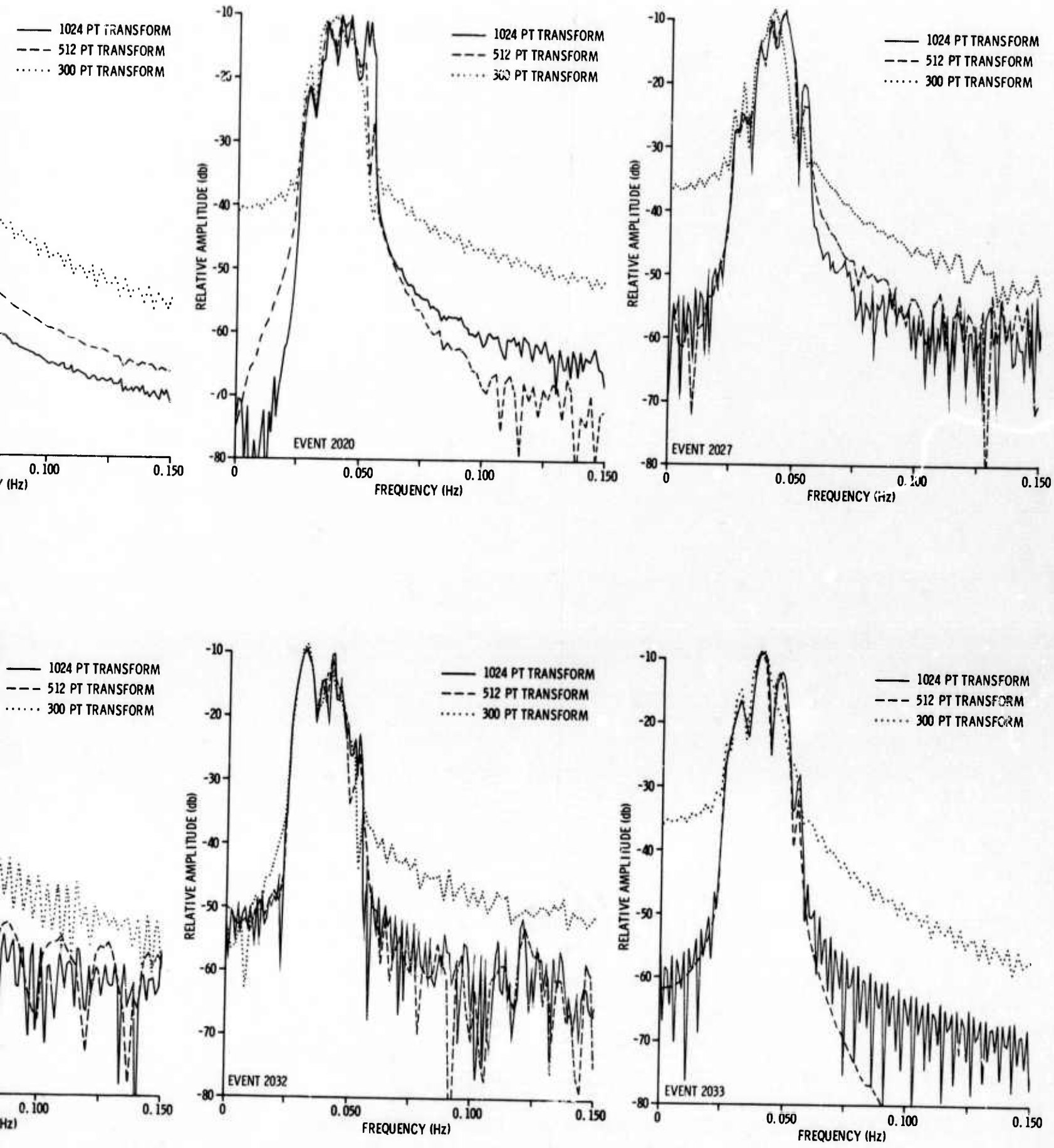

Figure III-3. Amplitude Spectra of Events as Seen Through the LASA LP Instrumentation. (Sheet 1 of 2)

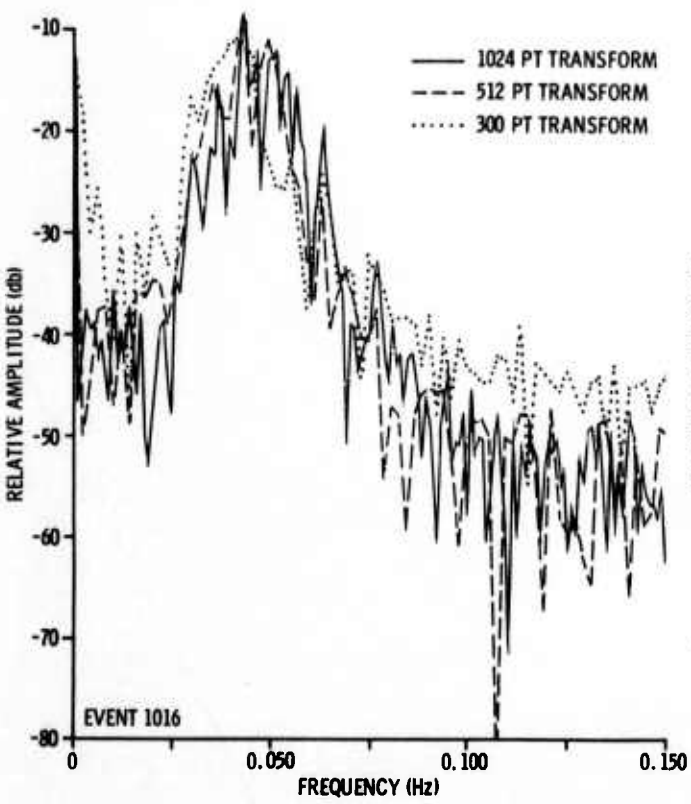
1024 PT TRANSFORM
512 PT TRANSFORM
300 PT TRANSFORM
RELATIVE AMPLITUDE (db)
-10
-20
-30
-40
-50
-60
-70
-80
EVENT 1016
0
0.050
0.100
0.150
FREQUENCY (Hz)

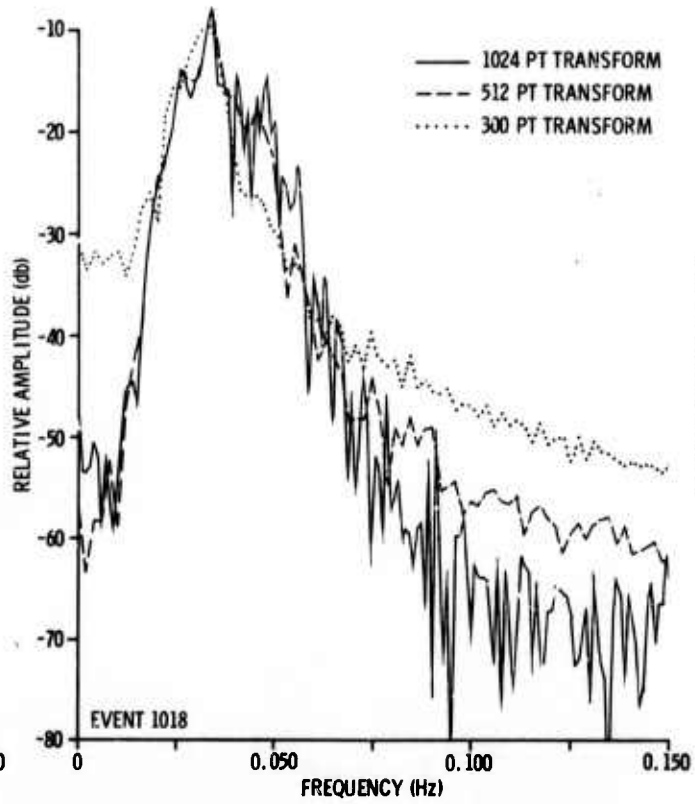
1024 PT TRANSFORM
512 PT TRANSFORM
300 PT TRANSFORM
RELATIVE AMPLITUDE (db)
-10
-20
-30
-40
-50
-60
-70
-80
EVENT 1018
0
0.050
0.100
0.150
FREQUENCY (Hz)

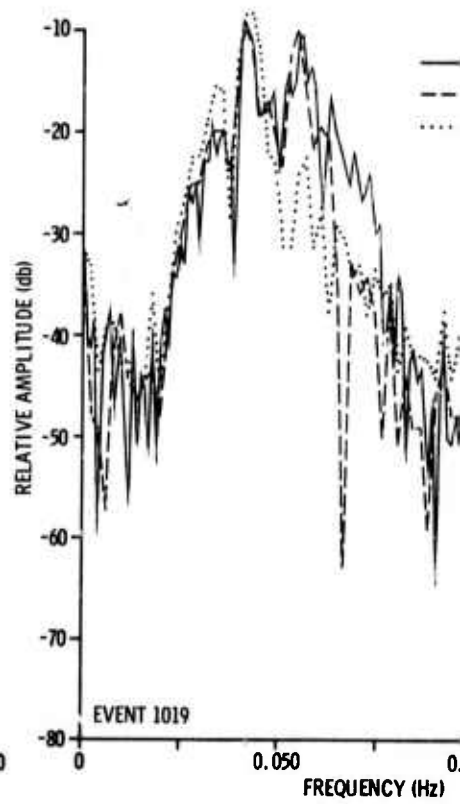
RELATIVE AMPLITUDE (db)
-10
-20
-30
-40
-50
-60
-70
-80
EVENT 1019
0
0.050
FREQUENCY (Hz)

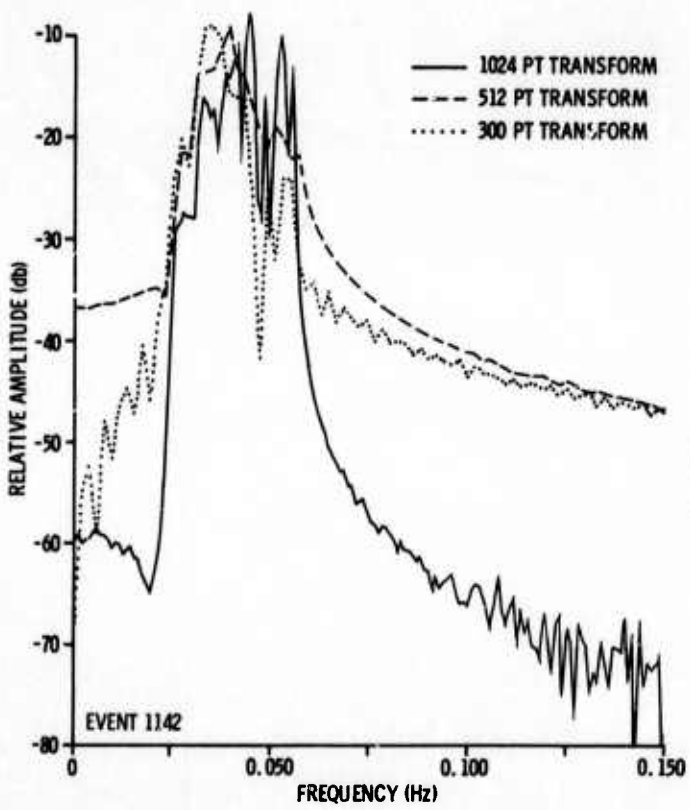
1024 PT TRANSFORM
512 PT TRANSFORM
300 PT TRANSFORM
RELATIVE AMPLITUDE (db)
-10
-20
-30
-40
-50
-60
-70
-80
EVENT 1142
0
0.050
0.100
0.150
FREQUENCY (Hz)

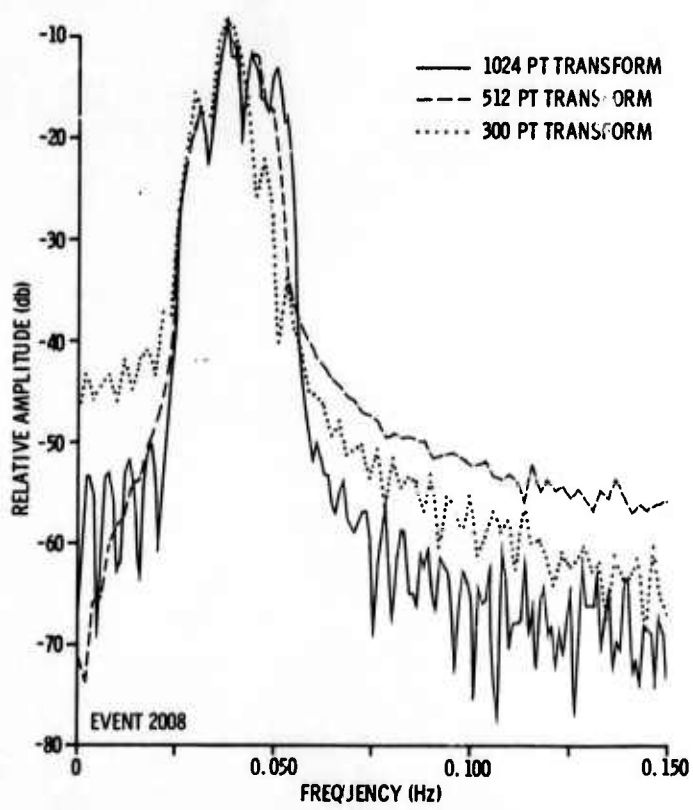
1024 PT TRANSFORM
512 PT TRANS ORM
300 PT TRANSFORM
RELATIVE AMPLITUDE (db)
-10
-20
-30
-40
-50
-60
-70
-80
EVENT 2008
0
0.050
0.100
0.150
FREQUENCY (Hz)

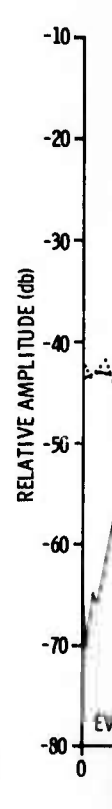
RELATIVE AMPLITUDE (db)
-10
-20
-30
-40
-50
-60
-70
-80
0

A

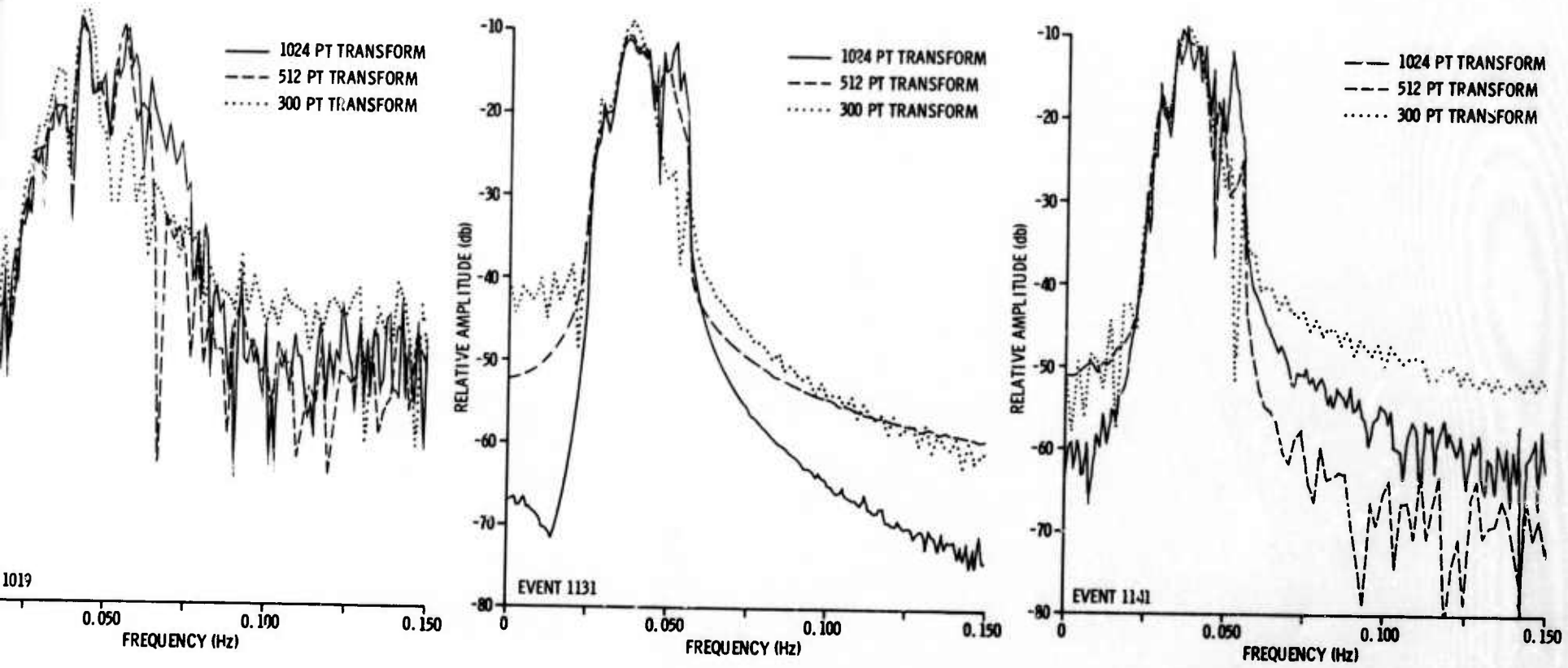

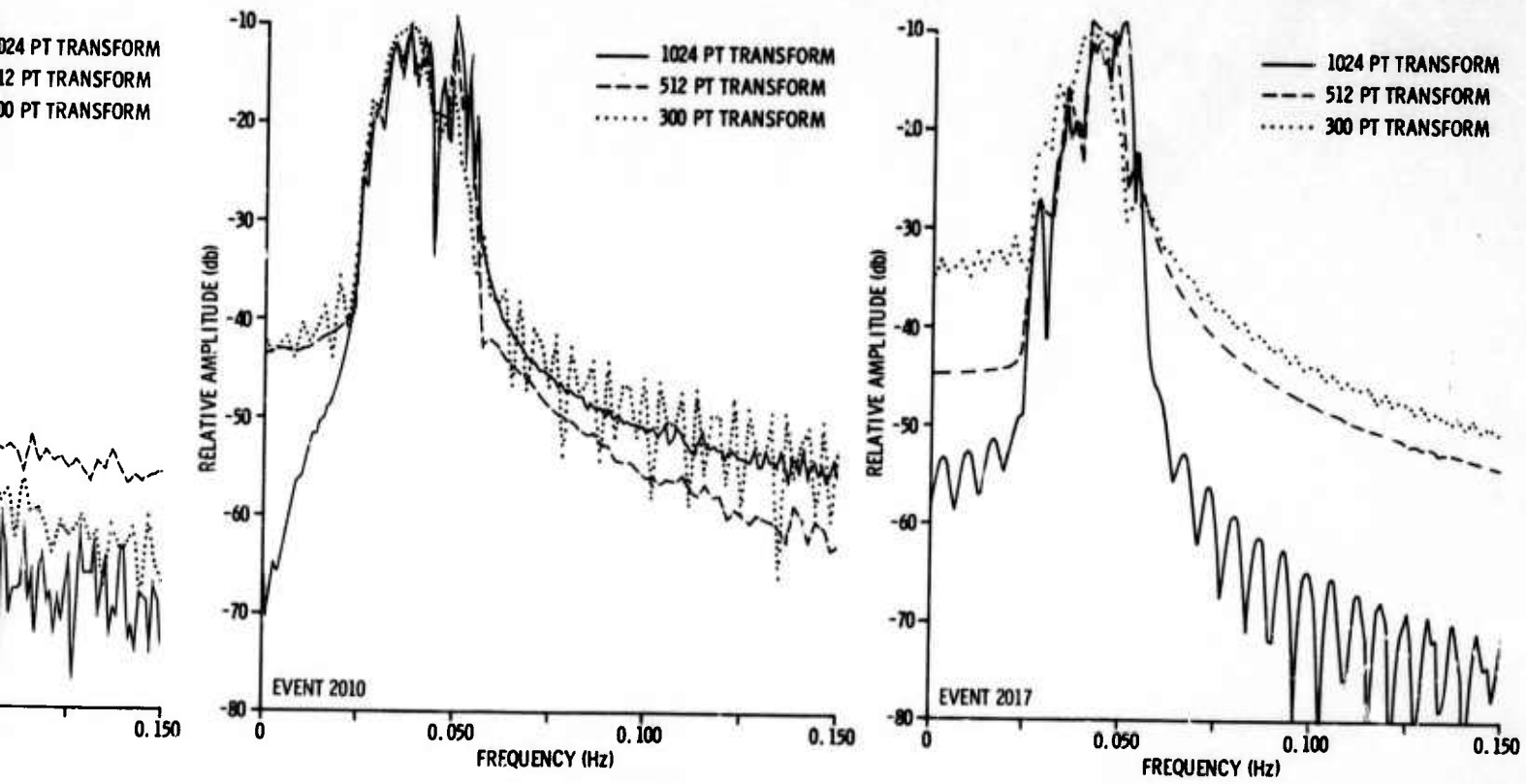

Figure III-3. (Sheet 2 of 2).

B

BLANK PAGE

SECTION IV

RESULTS

The matched filtering was done using events 1142, 2017, 2019, 2029 and 2033 as master events. These events were chosen to give a good spread of epicentral separations when used as the test event with each of the other 16 events. Table IV-1 gives the epicentral separation between the master events and the non-master events. The separation varies from 0 to 2216 km and a fairly good sampling of epicentral separations was obtained.

Also a chirp signal was used as a matching waveform as represented by the equation:

$$\text{Chirp Signal} = \sin\left\{2\pi\left[f_0 + \frac{(f_1 - f_0)\,t}{2T}\right]t\right\} \qquad \text{(IV-1)}$$

where:

$f_0 = 0.025$ Hz

$f_1 = 0.05$ Hz

$0 \leq t \leq T$ (Various values of T were used)

Finally, surface trains derived from published* dispersion curves for three different oceanic models were used. The amplitude spectra were flat from 0.025 Hz to 0.05 Hz and tapered off to zero on either end of this band. A Δ of 60 to 70° was used for each model, making a total of six such Rayleigh wavetrains.

It was originally intended to make several more complicated models using continental and oceanic in various reasonable path length combinations and assuming no phase distortion across the boundary. The results

---

* Saito, M., H. Takeuchi, 1966, Surface waves across the pacific: Bulletin of the Seismological Society of America, v. 56, No. 5, Oct., p. 1069-1078.

Table IV-1

EPICENTRAL DISTANCE SEPARATION (IN KM) BETWEEN MASTER AND OTHER EVENTS

	1142	2017	2019	2029	2033
1131	44	401	439	832	1164
1141	0	382	421	825	1157
1142	0	382	421	825	1157
2008	531	158	123	302	628
2010	339	135	155	572	888
2017	380	0	38	459	786
2018	473	100	68	359	687
2019	418	38	0	425	750
2020	252	152	188	570	902
2027	759	378	340	192	444
2028	331	55	92	497	827
2029	822	459	425	0	331
2032	1154	1197	1163	738	419
2033	1154	786	750	331	0
1016	244	137	175	593	922
1018	1062	1437	1475	1884	2216
1019	1388	1018	981	567	235

using the above models were so discouraging that it did not appear likely that any one crustal model would work appreciably better on the average than did Equation IV-1.

Figure IV-1 shows a plot of the correlation coefficients obtained using the first 300 seconds of both the master event and the test event using the equation

$$\text{correlation coefficients} = \left[\frac{\max_{T} \left| \sum_i f_1(t_i)\, f_2(t_i+T) \right|}{\left(\sum_i f_1^2(t_i) \sum_i f_2^2(t_i) \right)^{1/2}} \right] \qquad \text{(IV-2)}$$

The correlation coefficients are plotted against epicentral separation and coded to show which master event was being used. Table IV-2 lists the maximum value of each of the correlation functions and the lag at which it occurred. This same data is listed and shown for 512 seconds in Table IV-3 and Figure IV-2 and for 1024 seconds in Table IV-4 and Figure IV-3.

Figure IV-4 shows the correlation coefficients obtained using the various synthetic waveforms. The values for these coefficients are listed in Table IV-5.

Table IV-2

CORRELATION COEFFICIENTS AND LAG OF PEAKS
FOR MASTER EVENTS (FIRST 300 SECONDS)

	1142	2017	2019	2029	2033
1131	-0.869 -37	0.797 12	-0.793 44	0.886 -15	0.876 -22
1141	-0.884 -41	0.770 7	-0.787 40	0.872 -19	-0.856 -14
1142	1.0 0	-0.622 49	0.669 81	-0.798 22	0.677 27
2008	0.793 -32	0.708 30	0.747 49	0.847 3	0.938 -4
2010	-0.823 -39	-0.692 -3	0.747 29	0.797 -17	-0.807 -12
2017	-0.622 -49	1.0 0	-0.861 32	-0.830 -14	-0.801 -22
2018	0.728 -46	-0.919 3	0.869 35	-0.880 -24	-0.879 -32
2019	0.669 -81	0.861 -32	1.0 0	-0.846 -59	0.777 -54
2020	-0.744 -74	-0.867 -13	-0.878 7	-0.865 -39	-0.872 -47
2027	0.678 -73	0.868 -11	0.911 8	0.861 -38	0.871 -45
2028	-0.855 11	-0.638 72	-0.726 91	0.832 32	-0.772 38
2029	-0.798 -22	-0.830 14	-0.846 59	1.0 0	0.861 -8
2032	-0.508 13	0.528 -60	0.434 55	-0.516 21	0.686 -46
2033	0.677 -27	-0.801 22	0.777 54	0.861 8	1.0 0
1016	0.688 -42	-0.859 6	0.811 38	0.842 -8	0.837 -15
1018	0.599 73	0.305 105	0.378 124	0.497 79	-0.512 84
1019	-0.560 19	0.770 -27	0.847 -6	0.652 -53	-0.611 -49

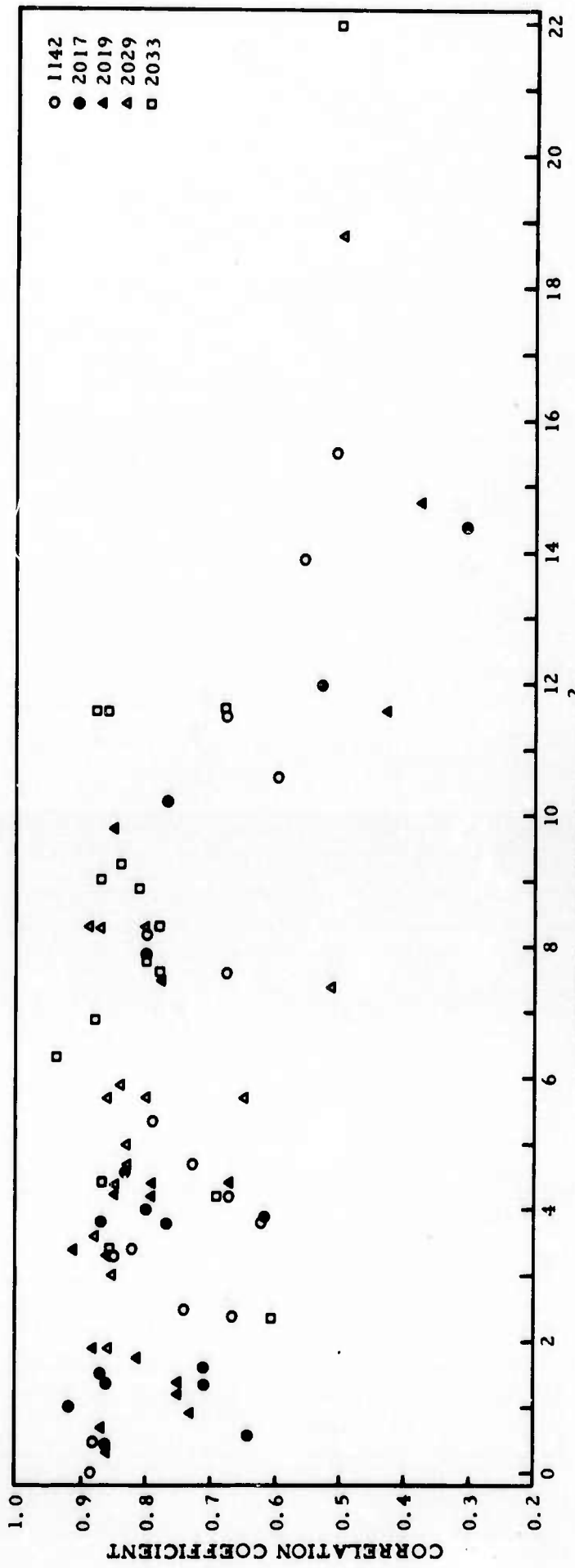

Figure IV-1. Correlation Coefficients of Events with Master Events (First 300 Seconds).

Table IV-3

CORRELATION COEFFICIENTS AND LAG OF PEAKS
FOR MASTER EVENTS (FIRST 512 SECONDS)

	1142	2017	2019	2029	2033
1131	0.658 -50	0.727 -1	0.799 31	0.666 11	-0.791 -9
1141	0.722 -55	0.614 [illegible]	0.713 27	-0.577 6	-0.777 -14
1142	1.0 0	-0.517 77	-0.521 121	0.434 -20	0.698 54
2008	0.666 -59	0.536 31	-0.649 62	-0.564 44	0.674 23
2010	0.591 -80	-0.635 23	0.693 55	-0.461 25	-0.511 15
2017	-0.517 -77	1.0 0	-0.918 32	-0.655 11	-0.600 2
2018	-0.581 -86	0.868 3	0.923 35	-0.482 27	-0.499 -6
2019	-0.521 -121	-0.918 -32	1.0 0	0.569 -20	-0.579 -41
2020	-0.644 -101	-0.859 -12	0.924 20	0.517 1	0.566 -33
2027	0.645 -100	0.728 -11	0.740 9	0.618 -10	-0.691 -31
2028	0.704 -3	0.625 86	0.747 105	0.422 87	0.685 52
2029	0.434 20	-0.655 -11	0.569 20	1.0 0	0.757 -8
2032	0.548 90	-0.476 -47	0.494 55	-0.367 21	0.550 -46
2033	0.698 -54	-0.600 -2	-0.579 41	0.757 8	1.0 0
1016	-0.396 108	0.763 7	-0.782 25	-0.520 5	0.451 -15
1018	0.586 44	-0.432 120	-0.508 140	0.474 108	0.634 99
1019	0.478 32	-0.608 -38	-0.563 -18	0.433 53	-0.518 -50

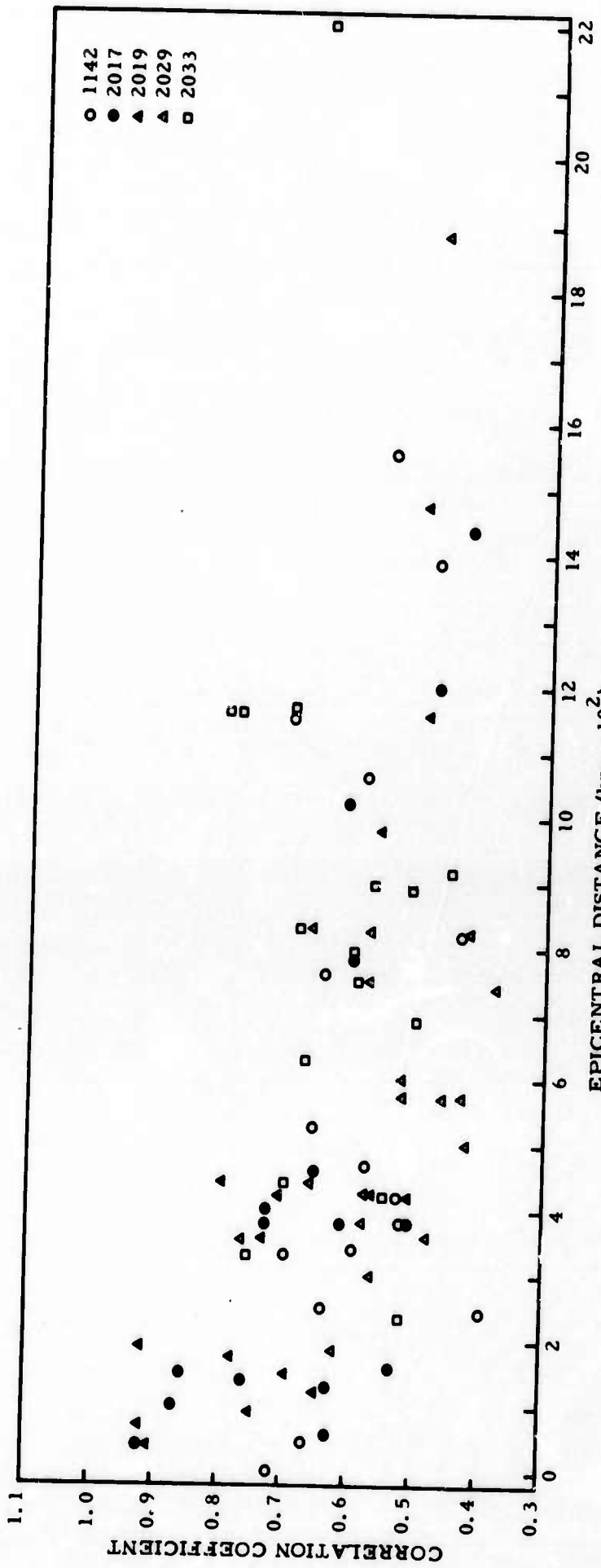

Figure IV-2. Correlation Coefficients of Events with Master Events (First 512 Seconds).

Table IV-4

CORRELATION COEFFICIENTS AND LAG OF PEAKS
FOR MASTER EVENTS (FIRST 1024 SECONDS)

	1142	2017	2019	2029	2033
1131	0.364 -78	0.646 -13	0.761 32	0.621 12	-0.713 3
1141	0.385 -83	0.497 -18	0.688 27	0.528 7	0.661 -2
1142	1.0 0	0.396 314	0.407 335	0.370 187	-0.444 80
2008	-0.518 -45	0.576 31	0.601 74	0.540 46	0.636 23
2010	-0.289 -38	-0.598 35	0.591 56	0.477 78	-0.464 2
2017	0.396 -314	1.0 0	0.712 44	0.506 65	-0.509 -9
2018	0.477 -75	-0.757 9	0.883 35	0.516 16	-0.443 18
2019	-0.407 -335	0.712 -44	1.0 0	0.606 -20	-0.512 -53
2020	0.529 -90	0.628 -25	0.930 20	0.564 1	0.497 -33
2027	0.487 -100	0.609 -11	0.654 9	0.561 -10	-0.686 -19
2028	-0.539 23	0.558 87	-0.536 131	0.364 113	-0.629 53
2029	0.370 -187	0.506 -65	0.606 20	1.0 0	0.671 -8
2032	0.307 91	0.393 -36	0.456 31	1.0 0	0.539 46
2033	-0.444 -80	-0.509 9	-0.512 53	0.671 8	1.0 0
1016	0.323 120	-0.465 -19	0.584 48	0.479 15	-0.343 -15
1018	0.418 72	0.363 107	-0.434 140	0.463 108	0.634 99
1019	0.334 -104	0.541 -50	0.459 -6	0.299 -53	-0.476 -50

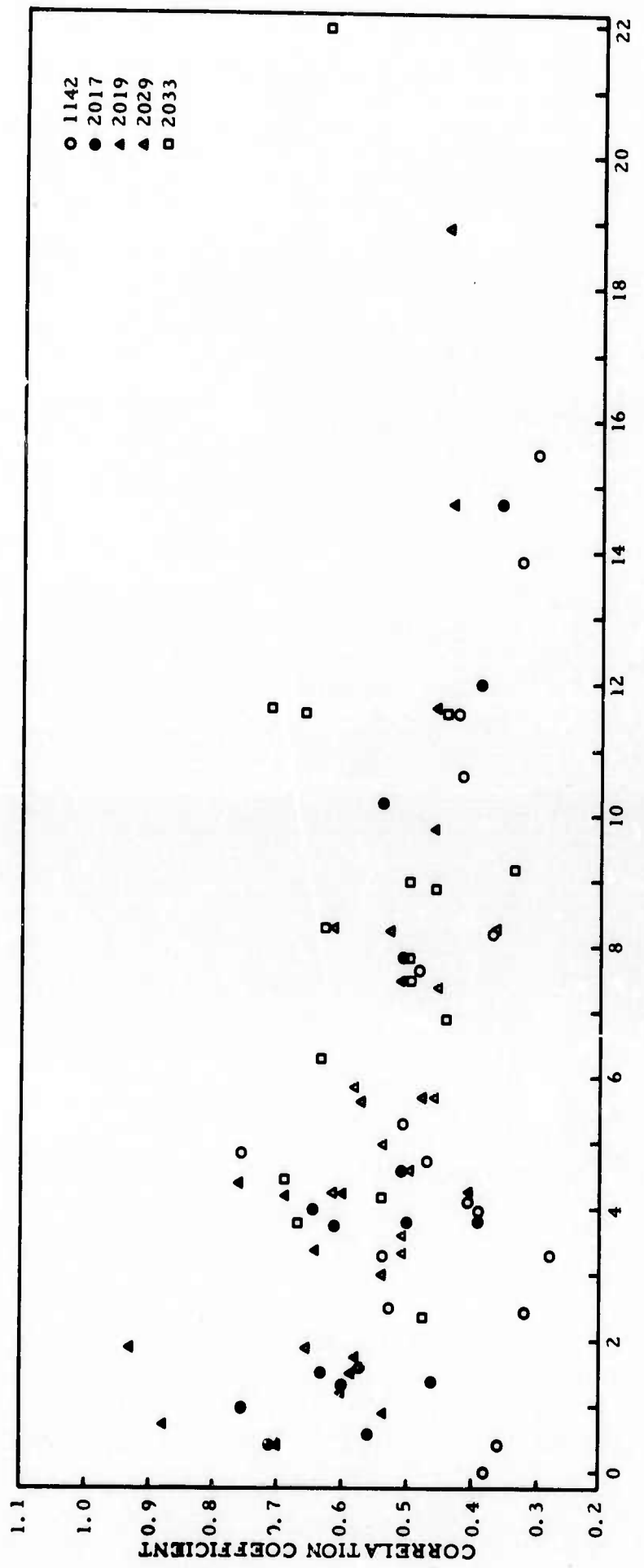

Figure IV-3. Correlation Coefficients of Events with Master Events (First 1024 Seconds).

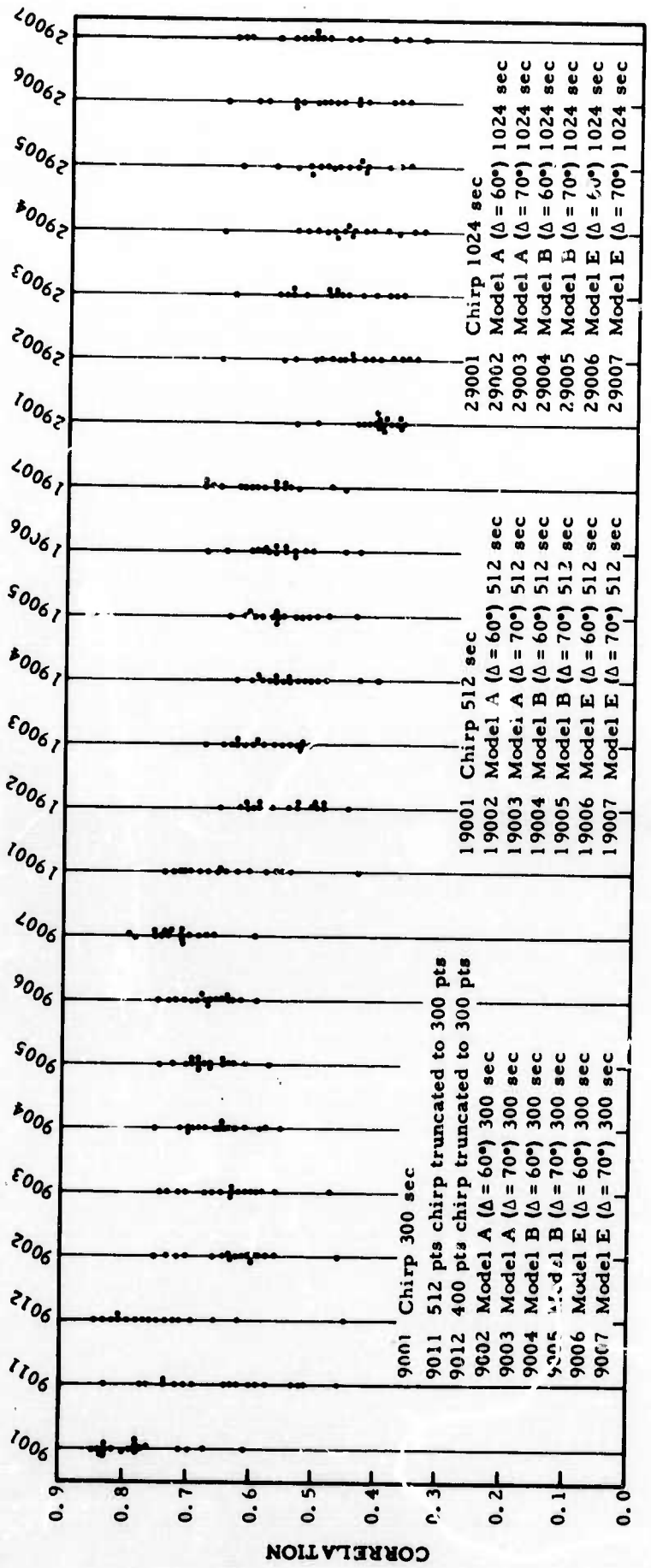

Figure IV-4. Correlation Coefficients Using Synthetic Waveforms (all 17 events).

Table IV-5

CORRELATION COEFFICIENTS AND LAG
USING SYNTHETIC WAVEFORMS (FIRST 300 SECONDS)

	9001	9002	9003	9004	9005	9006	9007
1131	-0.824 35	0.643 179	0.646 178	-0.651 161	0.644 14[illegible]	0.632 33	-0.706 13
1141	-0.828 30	0.623 174	-0.628 162	0.643 156	-0.646 141	-0.641 42	-0.710 8
1142	0.709 70	-0.610 217	0.622 202	0.645 197	-0.634 183	-0.593 96	0.596 74
2008	0.771 39	0.558 196	-0.563 159	0.583 140	0.633 138	0.654 51	0.710 17
2010	-0.811 32	-0.588 165	0.630 151	-0.679 133	-0.724 131	-0.750 45	-0.794 10
2017	-0.783 23	0.716 167	0.714 166	-0.717 149	-0.700 146	-0.651 59	0.658 13
2018	0.834 24	0.680 182	-0.669 169	0.688 150	-0.674 137	0.657 37	0.710 3
2019	-0.779 3	-0.733 147	0.733 135	-0.705 129	0.697 114	-0.694 16	-0.734 -19
2020	0.845 9	-0.661 156	-0.653 154	0.675 135	0.681 109	0.668 22	0.738 -12
2027	0.787 -1	0.725 156	0.727 155	-0.690 138	0.680 122	-0.621 48	-0.673 -10
2028	-0.749 81	0.572 201	0.598 200	-0.655 183	-0.678 181	-0.723 94	0.754 72
2029	-0.764 49	-0.752 182	-0.737 181	0.754 162	-0.746 148	-0.730 61	-0.736 28
2032	0.606 97	-0.613 191	-0.590 190	0.625 170	0.593 169	0.687 82	-0 693 62
2033	0.797 43	-0.593 214	-0.585 165	-0.612 159	0.665 143	0.684 56	0.731 22
1016	0.699 28	-0.457 185	0.469 160	0.551 143	-0.577 127	0.712 41	-0.754 7
1018	0.699 141	-0.457 235	0.469 219	0.551 214	-0.577 199	0.712 112	-0.754 106
1019	0.672 8	-0.579 131	0.608 116	-0.578 99	-0.610 97	-0.642 10	0.683 -13

Table IV-6

CORRELATION COEFFICIENTS AND LAG
USING SYNTHETIC WAVEFORMS (FIRST 512 SECONDS)

	19001	19002	19003	19004	19005	19006	19007
1131	0.688 -80	0.609 205	-0.679 192	0.592 173	0.620 171	0.570 84	0.586 50
1141	-0.624 -71	-0.600 189	0.627 174	0.602 168	-0.612 155	-0.576 43	0.614 21
1142	-0.706 -15	-0.534 245	0.571 230	0.568 225	-0.619 211	-0.591 124	0.600 101
2008	0.674 -61	0.449 196	0.479 222	0.491 140	0.531 138	0.540 51	0.567 17
2010	0.638 -55	-0.543 165	0.589 150	0.595 145	-0.643 131	-0.651 44	-0.683 10
2017	0.649 -92	0.573 192	-0.600 180	0.552 161	0.577 158	0.553 71	0.559 38
2018	-0.702 -88	-0.498 196	-0.523 195	-0.510 164	-0.502 162	0.454 86	-0.480 66
2019	-0.651 -123	-0.598 161	-0.623 160	-0.569 129	-0.570 127	-0.540 16	0.568 -6
2020	-0.739 -103	0.507 167	-0.535 180	0.524 135	0.528 109	-0.513 10	0.533 -12
2027	-0.714 -115	-0.595 170	-0.628 169	0.554 150	0.576 147	0.553 60	0.552 26
2028	0.727 -5	0.531 253	0.548 252	0.529 221	0.562 194	-0.588 95	0.623 73
2029	-0.607 -9	-0.616 194	-0.593 181	0.631 175	0.606 160	0.679 62	-0.660 39
2032	-0.607 76	-0.616 191	-0.593 190	0.631 170	0.606 168	0.679 81	-0.660 61
2033	0.543 -83	-0.651 214	0.640 200	0.582 194	-0.596 157	0.610 57	-0.682 36
1016	-0.552 -86	0.505 210	-0.554 198	-0.407 192	0.438 176	0.436 89	0.458 56
1018	0.563 102	-0.491 223	0.526 236	-0.506 255	-0.538 256	-0.585 144	0.677 122
1019	0.433 4	-0.493 131	0.529 117	0.430 111	0.484 108	-0.520 10	0.557 -13

Table IV-7

CORRELATION COEFFICIENTS AND LAG
USING SYNTHETIC WAVEFORMS (FIRST 1024 SECONDS)

	29001	29002	29003	29004	29005	29006	29007
1131	-0.369	-0.512	-0.553	0.485	0.508	0.512	0.526
	-375	194	193	173	171	84	50
1141	0.403	-0.473	0.479	-0.467	-0.476	-0.486	0.520
	-314	189	175	157	129	43	21
1142	0.374	-0.348	0.383	0.343	-0.376	-0.385	0.392
	-205	246	231	225	211	124	101
2008	0.440	-0.433	0.462	0.456	-0.482	0.497	0.523
	-262	161	145	140	126	51	17
2010	0.387	0.545	-0.565	-0.542	-0.573	-0.593	-0.624
	-198	152	139	134	132	44	10
2017	-0.412	0.422	-0.435	0.420	0.444	0.446	0.450
	-485	182	180	161	158	71	38
2018	-0.405	0.385	-0.384	-0.398	-0.394	-0.384	-0.397
	-373	183	196	164	162	75	66
2019	-0.391	-0.462	0.477	0.456	0.461	-0.468	0.494
	497	162	148	116	114	16	-6
2020	0.368	0.404	0.413	0.425	-0.439	-0.445	0.462
	-474	168	167	111	97	10	-12
2027	0.536	-0.541	-0.554	0.512	0.539	0.548	0.548
	-485	170	169	150	147	60	26
2028	-0.509	0.453	0.478	0.490	-0.522	-0.542	0.575
	-193	202	202	196	182	95	73
2029	0.398	-0.500	-0.528	0.463	0.494	-0.506	0.543
	-320	183	181	163	160	62	39
2032	0.423	-0.658	-0.640	0.663	0.634	0.658	-0.634
	-146	191	191	170	169	81	61
2033	0.439	-0.563	-0.553	0.534	0.575	0.606	-0.679
	-287	214	166	194	144	57	36
1016	0.406	-0.366	-0.377	0.351	0.358	0.363	-0.367
	-217	504	198	484	470	383	350
1018	-0.411	-0.478	-0.490	-0.478	0.489	-0.544	0.625
	-24	204	204	200	243	143	123
1019	-0.324	-0.416	0.466	0.380	-0.435	-0.471	0.502
	-412	131	117	111	97	10	-13

The features of this data are:

- The correlation functions using only the first part (300 sec) of the surface wavetrain are distinctly higher than those containing later arriving energy.
- A simple chirp waveform gives a correlation coefficient almost equal to those obtained using nearby master events when using only the first 300 seconds of the events.
- The correlation coefficient of the first 300 seconds of the Rayleigh wavetrain is apparently stable (chrip works well and master events work well to about 1000-km epicentral separation). The correlation coefficients using the later arriving energy are decidedly lower, and degrade rapidly with epicentral separation. The correlation coefficients using the entire Rayleigh wavetrain (1024 seconds) are low, highly scattered, and indeed some of them are not meaningful (i.e., essentially no more correlated than band limited random noise could reasonably be). This last point is obvious from considering the lag at which they occur as shown in Table IV-1.

A summary of the values of the average correlation coefficients given in Table IV-8 also illustrates these tendencies.

Table IV-8

AVERAGE CORRELATION COEFFICIENT

Chirp 300 Sec	0.77
Master Waveform 300 sec 0-200 Km Separation	0.81
Master Waveform 300 sec 200-400 Km Separation	0.76
Master Waveform 300 sec 400-600 Km Separation	0.79
Chirp 512 Sec	0.648
Master Waveform 512 sec 0-200 Km Separation	0.76
Master Waveform 512 sec 200-400 Km Separation	0.62
Master Waveform 512 sec 400-600 Km Separation	0.59

The peak of the matched filter output can be used directly as a discriminant which is related to surface wave magnitude.*,** The size of the peak, for a fixed-amplitude matched filter, is dependent upon the size of the arriving surface wave and the correlation between the wavetrain and the matching waveform. For the discriminant to be most useful it should be related closely to the size of the arriving surface wavetrain. For estimating surface wave size only – it is, therefore, desirable to use a matching waveform which gives as high a correlation coefficient as possible.

---

* Lincoln Lab Test Note 1967-50, 1967, Long-period signal processing results for large aperature seismic array, Nov. 15.

** Seismic Data Laboratory Report No. 175, 1967, Detection of surface waves from small events at teleseismic distances.

Based on the events studied,and with the above viewpoint in mind, the following matched filtering procedures would be reasonable:

- Use a simple chirp waveform of length somewhat less (say on the order of 3/4) than the expected length of a Rayleigh wavetrain from an impulsive source.
- Use the peak of the matched filter output, when statistically significant, directly as a discriminant related to surface wave energy. The assumption implicit in this procedure is that the correlation coefficient of the chirp with the Rayleigh wavetrain is the same for each event. Based on the events studied this does not seem to be an unreasonable assumption for the first 300 seconds of the data. It may be that the above assumption would not be reasonable in comparing events from widely separated locations.

The above discussion does not consider the S/N improvement available to matched filtering. The S/N improvement is proportional to the time-bandwidth product of the signal. It may therefore be a good strategy to use more than the first 300 seconds of the signal,which means accepting a lower and more variable correlation coefficient but gaining improved S/N ratio.

The S/N ratio was defined earlier by Equation II-2, and this is the same definition used in previous literature dealing with matched filtering of seismic signals. Used as a standard for comparison of S/N ratio in this report is a phaseless bandpass filter which passes a continuous band containing the main signal energy, and removes all energy outside this band. Such a filter could actually be approximated very simply in operation by using a bank of bandpass filters and taking the output which appears to give the best S/N ratio.

The difference between the bandpass filter and the matched filter is that the matched filter has a phase which is designed to try to duplicate that phase of the signal which causes the signal energy to add coherently and peak. Additionally, like the zero-phase filter, it is a bandpass filter.

The gain of the matched filter over the zero-phase filter is a function of:

- Nonuniformity of the wavetrain (i.e., relationship between peak-value-squared and mean-squared-value)
- Time duration of the signal (if only the first part of the signal is used some potential S/N improvement is obviously sacrificed)
- Bandwidth of the signal
- Correlation coefficient between the matching waveform and the subject signal

Figure IV-5 shows the S/N improvements relative to bandpass filtering as a function of epicentral separation obtained using the five master events. These were obtained using only the first 300 seconds of the analysis gate. These S/N improvements were calculated assuming that the noise spectrum was flat over the band of signal energy (about 0.025 to 0.05 Hz). The numerical values of the numbers plotted in Figure IV-5 are listed in Table IV-9.

This same data is shown in figures IV-6 and IV-7 and listed in tables IV-10 and IV-11 for the 512 and 1024 seconds of signals respectively.

Figure IV-8 shows the S/N improvements obtained using a representative group of synthetic waveforms and table IV-12 lists the numerical values. Waveforms which were inferior, or not appreciably different (on the average), were omitted from this plot.

The S/N improvements that could have been obtained with the correct matching waveform —the signal itself— is listed in Table IV-13.

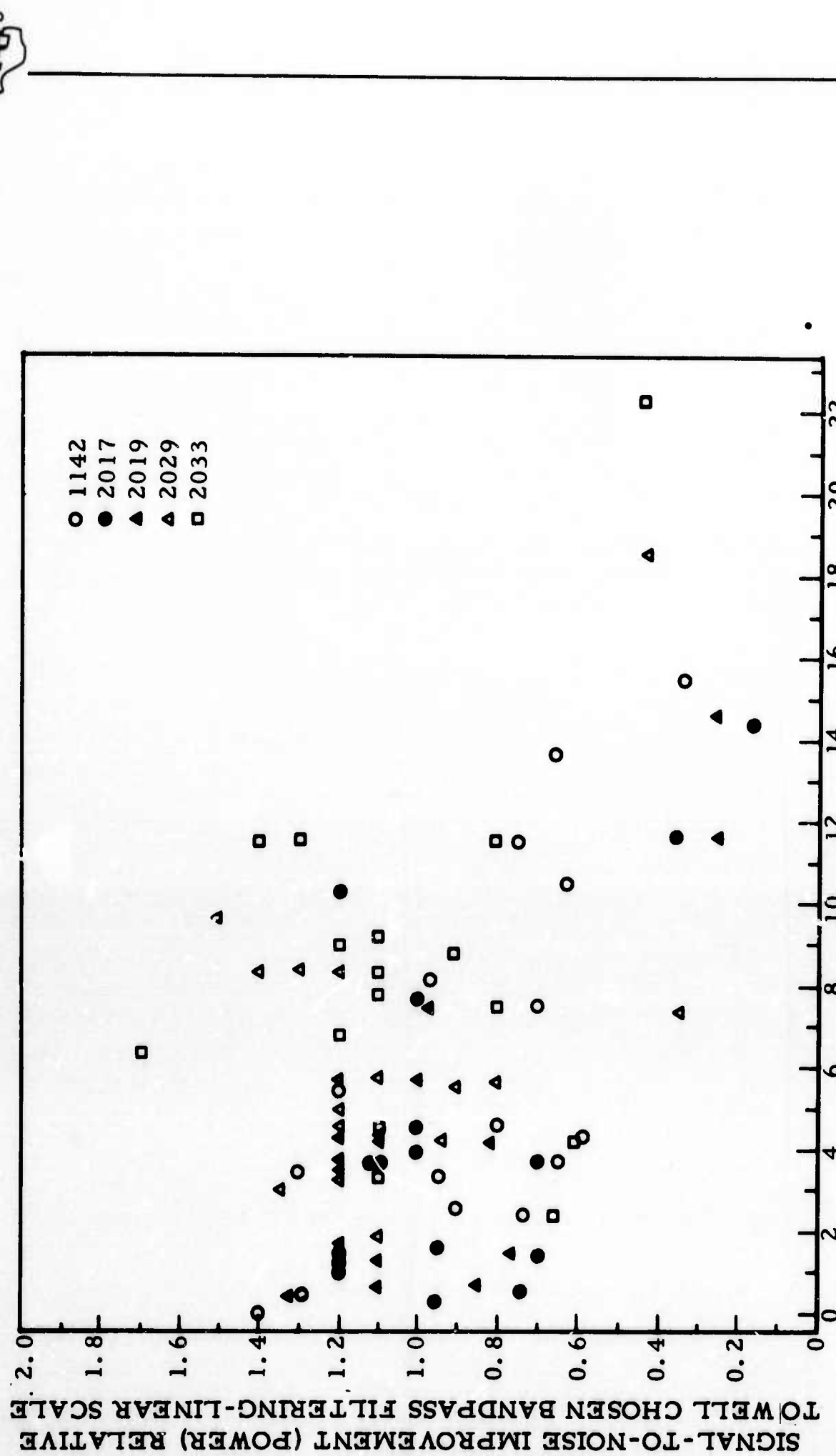

Figure IV-5. S/N Improvement as a Function of Epicentral Separation (For 300 Seconds).

Table IV-9

S/N IMPROVEMENT AS A FUNCTION OF EPICENTRAL SEPARATION
(FOR 300 SECONDS)

	1142	2017	2019	2029	2033
1131	1.3	1.0	1.1	1.3	1.3
1141	1.4	1.1	1.2	1.4	1.4
1142	1.8	0.70	0.81	1.2	0.81
2008	1.2	0.95	1.1	1.3	1.7
2010	0.94	0.70	0.78	0.90	0.91
2017	0.65	1.7	1.3	1.2	1.1
2018	0.80	1.2	1.1	1.2	1.2
2019	0.59	0.96	1.3	0.94	0.80
2020	0.88	1.2	1.2	1.2	1.2
2027	0.69	1.1	1.2	1.1	1.1
2028	1.3	0.74	0.85	1.2	1.1
2029	0.96	1.0	1.1	1.5	1.1
2032	0.34	0.37	0.25	0.35	0.61
2033	0.74	1.0	0.97	1.2	1.6
1016	0.75	1.2	1.0	1.1	1.1
1018	0.61	0.17	0.25	0.43	0.44
1019	0.65	1.2	1.5	0.88	0.67

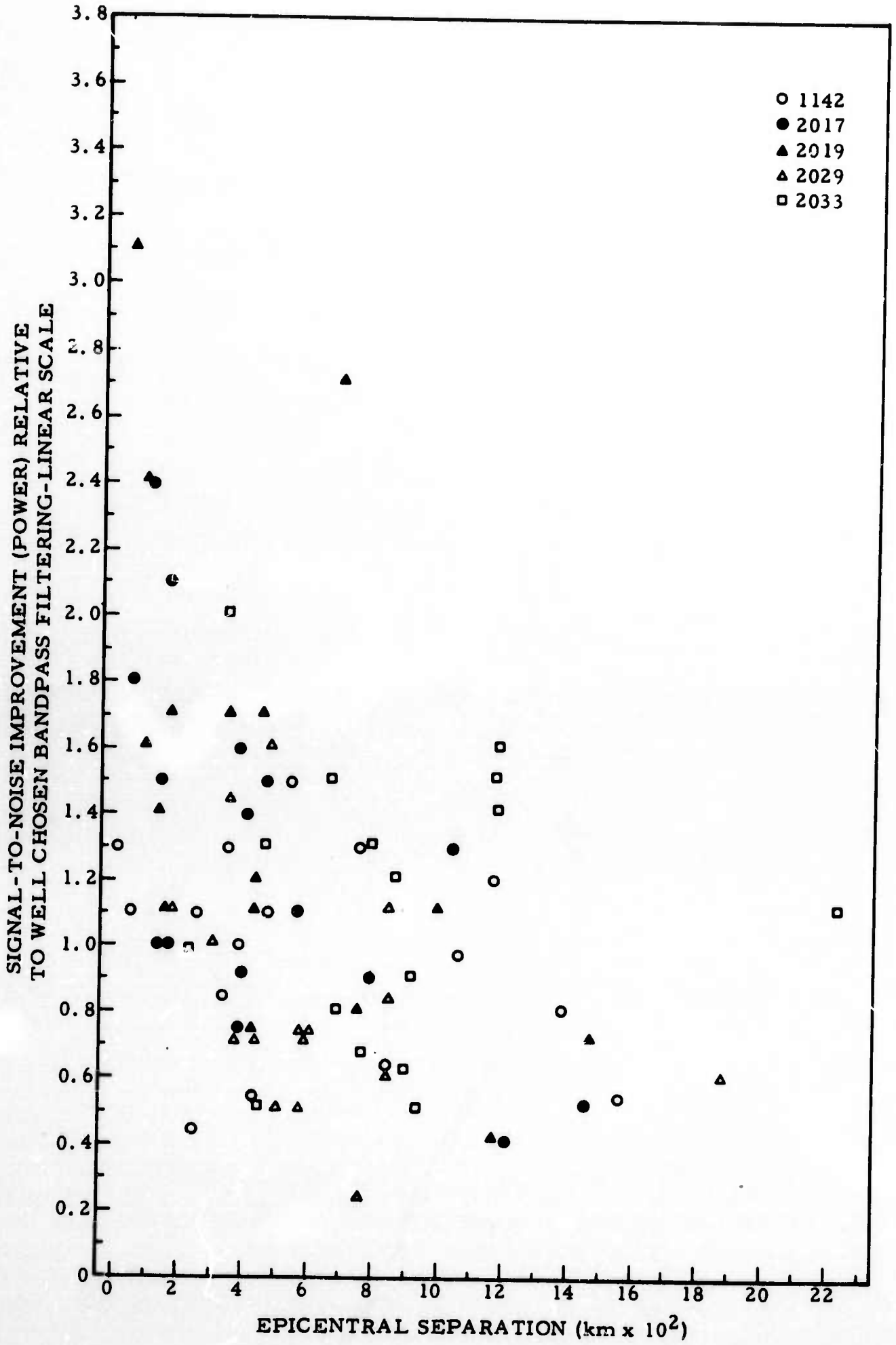

Figure IV-6. S/N Improvements as a Function of Epicentral Distances Using Master Events' Signals for 512 Seconds.

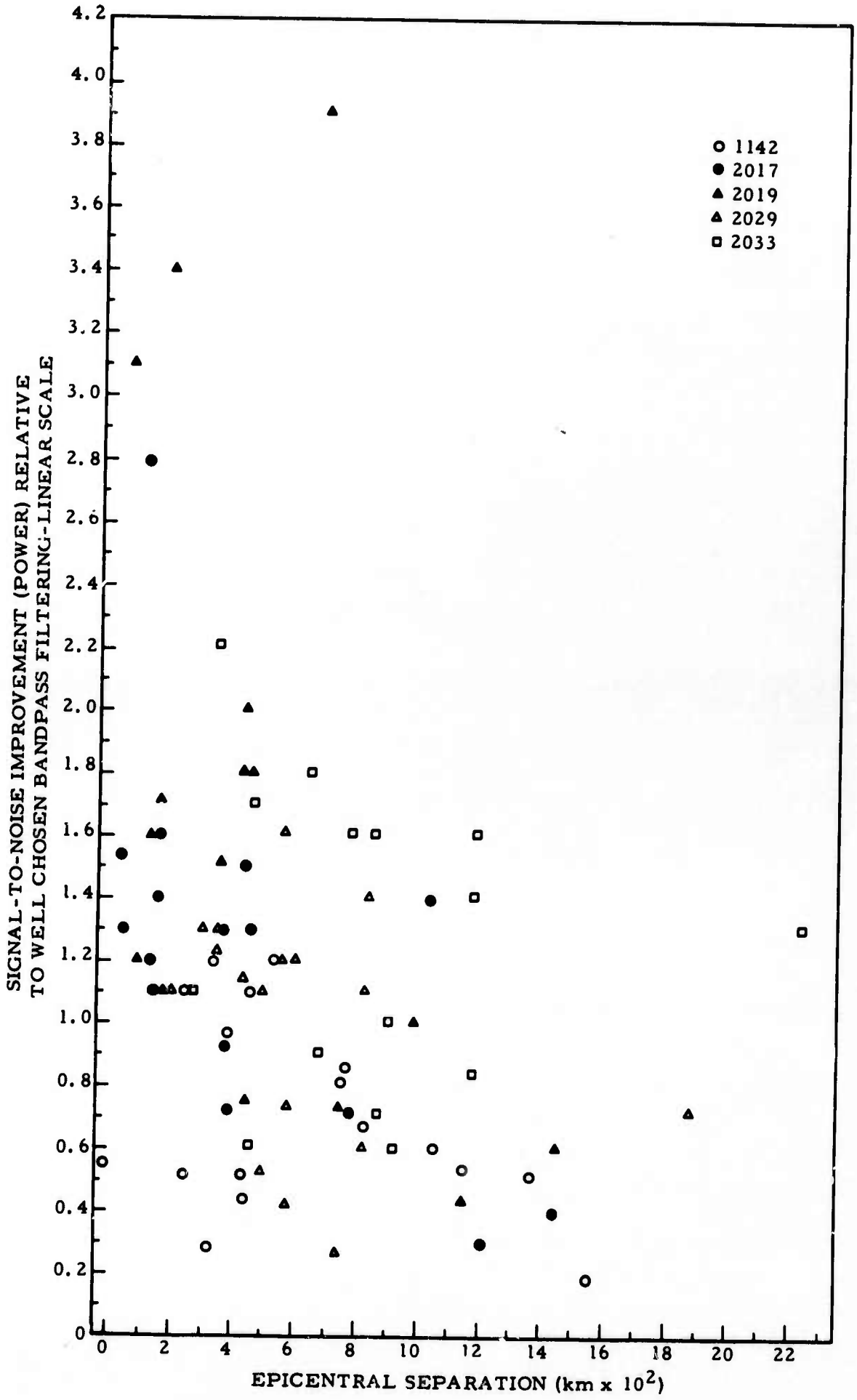

Figure IV-7. S/N Improvements as a Function of Epicentral Distances Using Master Events' Signals for 1024 Seconds.

Table IV-10

S/N IMPROVEMENTS AS A FUNCTION OF EPICENTRAL DISTANCES USING MASTER EVENTS' SIGNALS FOR 512 SECONDS

	1142	2017	2019	2029	2033
1131	1.1	1.4	1.7	1.1	1.6
1141	1.3	0.93	1.2	0.85	1.5
1142	2.8	0.76	0.76	0.59	1.4
2008	1.5	1.0	1.4	1.0	1.5
2010	0.87	1.0	1.1	0.50	0.62
2017	1.0	3.7	3.1	1.6	1.3
2018	1.1	2.4	2.7	0.74	0.80
2019	0.57	1.8	2.1	0.67	0.69
2020	1.1	2.1	2.4	0.75	0.90
2027	1.3	1.6	1.7	1.1	1.3
2028	1.3	1.3	1.6	0.52	1.2
2029	0.66	1.5	1.1	3.5	2.0
2032	0.54	0.41	0.43	0.25	0.54
2033	1.22	0.90	0.83	1.45	2.5
1016	0.45	1.5	1.7	0.76	0.53
1018	0.98	0.53	0.73	0.61	1.1
1019	0.83	1.3	1.1	0.68	0.97

Table IV-11

S/N IMPROVEMENTS AS A FUNCTION OF EPICENTRAL DISTANCES USING MASTER EVENTS' SIGNALS FOR 1024 SECONDS

	1142	2017	2019	2029	2033
1131	0.47	1.5	2.0	1.4	1.6
1141	0.56	0.93	1.8	1.1	1.4
1142	4.5	0.72	0.77	0.63	0.85
2008	1.2	1.4	1.6	1.3	1.8
2010	0.29	1.2	1.1	0.74	0.67
2017	0.98	6.1	3.1	1.6	1.6
2018	1.1	2.8	3.9	1.3	0.93
2019	0.53	1.55	3.1	1.15	0.81
2020	1.1	1.6	3.4	1.2	1.
2027	0.86	1.3	1.5	1.1	1.
2028	1.2	1.3	1.2	0.53	1.6
2029	0.68	1.3	1.8	4.9	2.2
2032	0.2	0.32	0.44	0.29	0.61
2033	0.53	0.73	0.73	1.26	2.8
1016	0.51	1.1	1.7	1.2	0.61
1018	0.61	0.44	0.61	0.72	1.3
1019	0.52	1.4	1.0	0.42	1.1

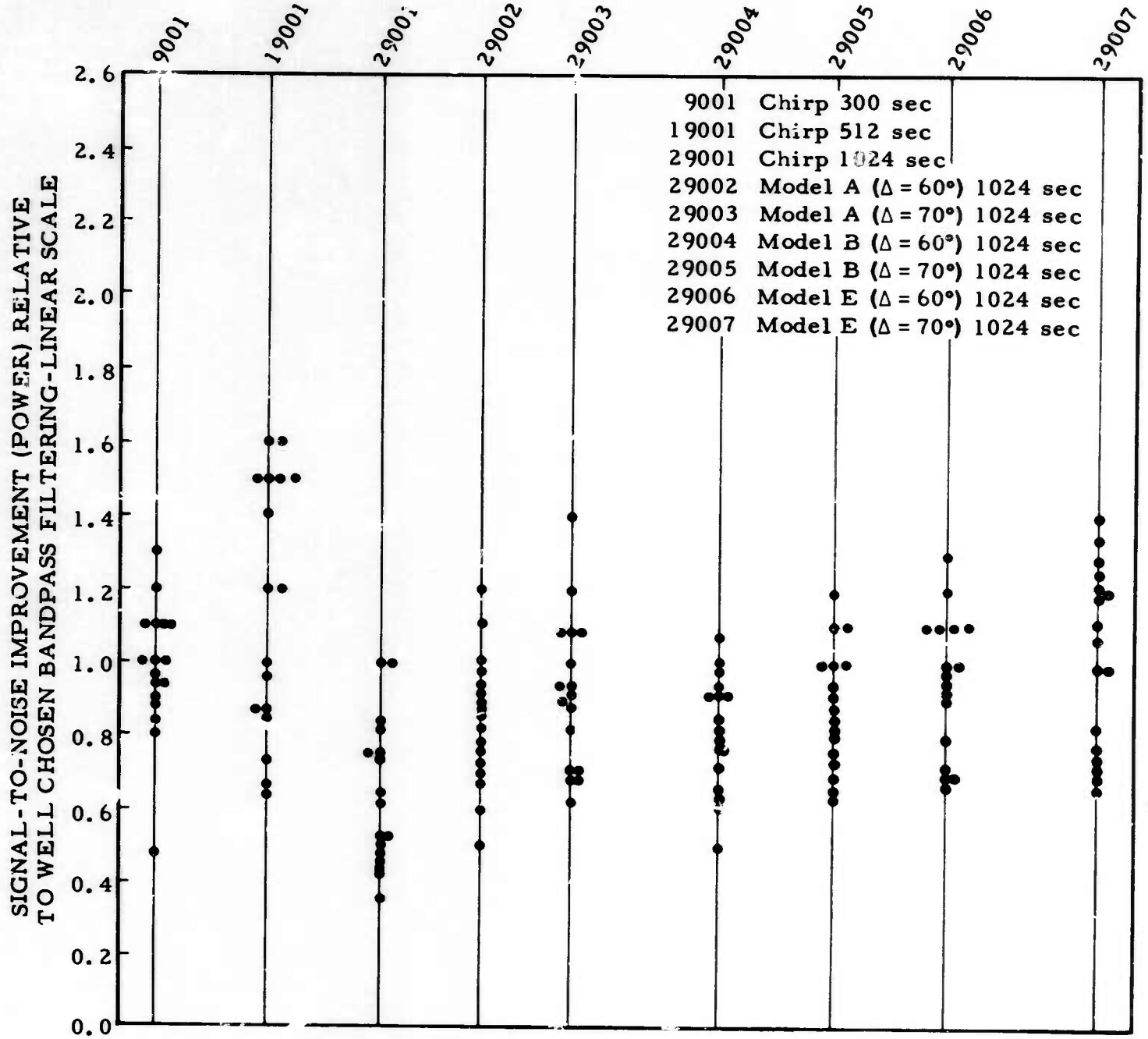

Figure IV-8. S/N Improvements for Synthetic Matching Waveforms.

Table IV-12

S/N IMPROVEMENTS FOR SYNTHETIC MATCHING WAVEFORMS

	9001	19001	29001	29002	29003	29004	29005	29006	29007
1131	1.1	1.2	504	936	1.080	864	936	936	1.008
1141	1.3	0.97	608	836	874	836	874	912	1.026
1142	0.90	1.4	0.63	0.54	0.63	0.54	0.63	0.67	0.67
2008	1.1	1.5	836	792	924	924	1.012	1.100	1.188
2010	0.93	1.0	480	960	1.024	928	1.024	1.120	1.248
2017	1.0	1.5	1.037	1.098	1.159	1.098	1.159	1.220	1.220
2018	1.0	1.6	784	735	686	784	735	686	784
2019	0.8	0.88	0.47	0.65	0.71	0.65	0.65	0.68	0.74
2020	1.2	1.5	560	600	680	720	760	800	840
2027	0.93	1.6	1.044	1.044	1.080	936	1.044	1.080	1.080
2028	1.1	1.5	1.066	820	943	984	1.107	1.148	1.394
2029	0.88	1.2	784	1.225	1.372	1.029	1.176	1.274	1.421
2032	0.48	0.67	378	924	861	924	840	924	735
2033	1.0	0.73	0.53	0.90	0.84	0.78	0.95	1.04	1.29
1016	1.1	0.84	867	714	714	612	663	663	714
1018	0.83	0.87	578	782	816	782	816	986	1.360
1019	0.95	0.65	470	846	1.034	658	893	1.034	1.175

Table IV-13

S/N IMPROVEMENTS (POWER NOT IN DB) USING THE EVENT ITSELF AS THE MATCHING FILTER

Event	300 Seconds	512 Seconds	1024 Seconds
1131	1.7	2.6	3.6
1141	1.9	2.5	3.8
1142	1.8	2.8	4.5
2008	1.9	3.4	4.4
2010	1.4	2.4	3.2
2017q	1.7	3.7	6.1
2018	1.5	3.2	4.9
2019	1.3	2.1	3.1
2020	1.6	2.8	4.0
2027	1.5	3.1	3.6
2028	1.8	2.9	4.1
2029	1.5	3.5	4.9
2032	1.3	1.8	2.1
2033	1.6	2.5	2.8
1016	1.6	2.8	5.1
1018	1.7	2.8	3.4
1019	1.7	3.6	4.7
Uniform Amplitude Event With Same Bandwidth	4.4	9.6	21.2

These data have several important features:

- The signals do not offer the possibility of large gains in S/N ratio. It can be seen, by the data listed in table IV-13, that the S/N improvements available with perfect matching average: 1.6 (2db) for 300 seconds, 2.85 (4.5db) for 512 seconds, and 4.0 (6db) for 1024 seconds. The 1024 seconds includes essentially all the signal energy in every case. These low figures occur basically because the square of the peak-signal-excursion is large relative to twice the mean-square-signal value. For a uniform wavetrain the square of the maximum excursion would be about twice the mean squared value of the wavetrain. This would result in a S/N improvement of about: 4.4 (6.4db) for the first 300 seconds of data or 9.6 (9.8db) for 512 seconds of data

- The S/N results actually realized using the first 300 seconds of data are not much different than bandpass filtering on the average

- In order to use some of the later arriving energy (512 or 1024 seconds), it is necessary to have a master event very near. Otherwise there is a good chance of considerable S/N loss. For this data the average S/N improvement factor, using master events within 200 km, was: 1.67 for the first 512 seconds and 1.71 for the first 1024 seconds. There were no examples of S/N loss using 512 points and only 2 examples of loss using 1024 points. The synthetic waveforms give significantly poorer results than nearby master events on the 512-second and especially on the 1024-second data

- Unlike the data using only 300 points, the S/N improvements, using master events and a longer piece of the wavetrain, decay rapidly with increase in the epicentral separation. It appears to be very difficult to obtain the S/N improvements inherently available in a elongated wavetrain. (e.g., A 6.1(7.9db) gain would be possible with an exact match to the entire wavetrain of event 2017, but the master events give the improvements shown in **Table IV-14.**

Table IV-14

MASTER EVENTS S/N IMPROVEMENTS
FOR EVENT 2017

Master Event No.	Epicentral Separation (km)	Gain Factor (Linear)
1142	380	0.98
2019	38	3.1
2029	459	1.6
2033	786	1.6

SECTION V

CONCLUSIONS

Although redundant, it is felt that it is worthwhile to repeat the significant features of the signals studied before presenting the conclusions. These features are:

- Events were recorded at LASA from the Kuriles region and, therefore, traveled a path along the continent-ocean basin boundary. This path might well be subject to complex multipathing, thereby resulting in unusually modulated (nonuniform) wavetrains and wavetrains which varied quite rapidly as a function of epicenter. Both of these effects are seriously detrimental to matched filtering. To illustrate this further group velocity curves calculated from events 2017 and 2018 are shown in Figure V-1.

  Not only are these group velocity plots complex but they are rather different, even though the events are separated by only 100 Km. Many of the events gave a group velocity plots which were more scattered and complex than these.

  By contrast, a group velocity plot is shown for an event from the South Pacific. For events from this region and most other regions, the group velocity plots cluster along a smooth, respectable curve.

- The events studied were generally band limited to the 0.025- to 0.05-Hz range. However, other studies* indicate that LP surface phases routinely recorded have a somewhat broader bandwidth. In such a case the increased S/N improvement available to match filtering is directly proportional to the signal bandwidth.

* Pomeroy, et al, 1969, Preliminary results from high-gain, wide-band, long-period electromagnetic seismograph systems: Journal of Geophysical Research, v. 74, No. 12, June 15.

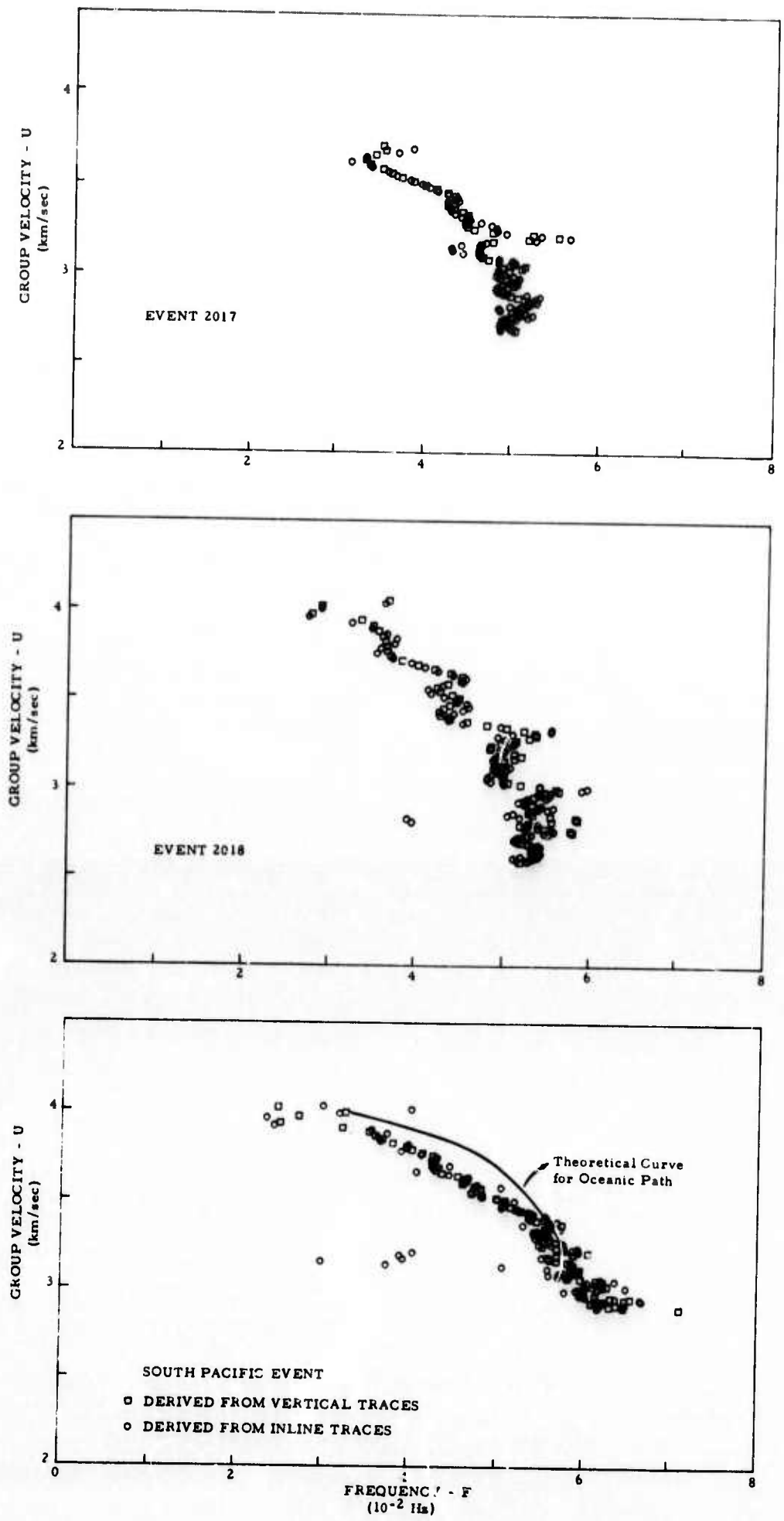

Figure V-1. Group Velocity Vs Frequency Plots

The following conclusions are made as a result of data presented in this report.

For the signals studied from the Kuriles, routine matched filtering at LASA does not appear to be a very powerful tool. Two routine methods of operation appear reasonable.

Since the output of the matched filtering operation can be used directly as a discriminant related to the total energy in the wavetrain* (in a fixed region at least), it would be desirable to make this measurement using a matching filter which would give a high correlation coefficient with most events. The signals analyzed indicate that this could be accomplished by using only about 3/4 of the expected duration of a simple event and employing either a fairly close (800 km) master event or a simple chirp waveform. Both of these gave average correlation coefficients on the order of 0.8. There were not sufficient signals processed to give a good estimate of the variability of such a procedure, but an assumption of equal correlation with each event does not appear to be unreasonable.

This procedure would only give S/N improvement comparable to a narrow band filter, but it would give an output which would be more useful for discrimination purposes. It will be recalled that the bandpass filter does not compress the waveform; therefore, a comparable S/N ratio means that the maximum excursion of the bandpassed signal would be about as visible in the noise as the peak of the matched filter output. A characterization of the surface wavetrain, using the matched filtered peak, would generally be preferred to information on the size of the maximum excursion.

---

* Seismic Data Laboratory Report No. 175, 1967, Detection of surface waves from small events at teleseismic distances.

If it is desired to improve upon the above procedure it would require a close (within about 200 km) master event. Using such a master event and the entire, or nearly the entire, wavetrain, a small S/N improvement (a factor of about 1.7 or 2.3 db) was obtained. The average correlation coefficient was 0.755 for 512 seconds using master events within 200 km. This is comparable to what could be obtained using a chirp wave form and 300 seconds (0.77). Again, there was insufficient data to make a really meaningful estimate of the variability of these correlation coefficients.

It is recommended that the above procedures be implemented initially in the off-line, long-period, analysis package at SAAC. After an accumulation of a more significant data base these procedures should be re-evaluated on a regional basis.

UNCLASSIFIED
Security Classification

DOCUMENT CONTROL DATA - R & D

(Security classification of title, body of abstract and indexing annotation must be entered when the overall report is classified)

1. ORIGINATING ACTIVITY *(Corporate author)*
Texas Instruments Incorporated
Services Group
P.O. Box 5621, Dallas, Texas 75222

2a. REPORT SECURITY CLASSIFICATION
Unclassified

2b. GROUP
—

3. REPORT TITLE
A PRELIMINARY STUDY OF TECHNIQUES FOR ROUTINE MATCHED FILTERING OF SURFACE WAVES
SEISMIC ARRAY PROCESSING TECHNIQUES TECH. RPT. NO. 4

4. DESCRIPTIVE NOTES *(Type of report and inclusive dates)*
Technical

5. AUTHOR(S) *(First name, middle initial, last name)*
Frank H. Binder

6. REPORT DATE
27 April 1970

7a. TOTAL NO. OF PAGES
47

7b. NO. OF REFS
4

8a. CONTRACT OR GRANT NO.
F33657-70-C-0100

b. PROJECT NO.
VELA/T/0701/B/ASD

c.

d.

9a. ORIGINATOR'S REPORT NUMBER(S)
—

9b. OTHER REPORT NO(S) *(Any other numbers that may be assigned this report)*
—

10. DISTRIBUTION STATEMENT
This document is subject to special export controls and each transmittal to foreign governments or foreign nationals may be made only with prior approval of Chief, AFTAC.

11. SUPPLEMENTARY NOTES
ARPA Order No. 624

12. SPONSORING MILITARY ACTIVITY
Advanced Research Projects Agency
Department of Defense
The Pentagon, Washington, D. C. 20301

13. ABSTRACT

This report discusses the study made on the effectiveness of various matched filters for processing surface waves of events in the Kuriles as recorded at LASA. The correlation coefficients and signal-to-noise improvements are presented for matching waveforms which include master events, a chirp waveform, and waveforms generated from crustal models. Based on the results of this study, procedures are recommended for implementation of large scale matched filtering at the SAAC center.

DD FORM 1 NOV 65 1473

UNCLASSIFIED
Security Classification

14. KEY WORDS	LINK A		LINK B		LINK C	
	ROLE	WT	ROLE	WT	ROLE	WT
Matched Filtering						
Surface Wave						